

Sl. No.	<p style="text-align: center;"><b>IIT Ropar</b>  <b>List of Recent Publications with Abstract</b>  <b>Coverage: July, 2022</b></p>
1.	<p><a href="#">3D Multi-voxel Pattern Based Machine Learning for Multi-center fMRI Data Normalization</a>  AJ Thomas, DR Bathula - International Conference on Computer Vision and Image Processing, 2022</p> <p><b>Abstract:</b> Multi-center fMRI studies help accumulate significant number of subjects to increase the statistical power of data analyses. However, the seemingly ambitious gain is hindered by the fact that differences between centers have significant effects on the imaging results. We present a novel machine learning (ML) based technique, which uses non-linear regression with multi-voxel based anatomically informed contextual information, to help normalize multi-center fMRI data to a chosen reference center. Accuracy graphs were obtained by thresholding the estimated maps at high p-values of <math>p &lt; 0.001</math> after kernel density estimation. Results indicate significant reduction in spurious activations and more importantly, enhancement of the genuine activation clusters. Group level ROI based analysis reveals changes in activation pattern of clusters that are consistent with their role in cognitive function. Furthermore, as the mapping functions exhibit the tendency to induce sensitivity to the regions associated with the task they can help identify small but significant activations which could otherwise be lost due to population based inferences across centers.</p>
2.	<p><a href="#">A computationally efficient <math>C^0</math> continuous finite element model for thermo-mechanical analysis of cross-ply and angle-ply composite plates in non-polynomial axiomatic framework</a>  YS Joshan, A Soni, N Grover - The Journal of Strain Analysis for Engineering Design, 2022</p> <p><b>Abstract:</b> In the present article, the thermo-mechanical bending response of multi-layered composite plates is investigated in the framework of inverse-hyperbolic shear deformation theory using a generalized finite element model. The mathematical development is carried out under the assumptions of linear structural kinematics for the materials following generalized Hooke's law. Energy-based finite element formulation and the principle of minimum potential energy are employed to develop the finite element governing equations. A computationally efficient <math>C^0</math> continuous finite element formulation is developed to examine the response of laminated composites subjected to constant, linear, and non-linear temperature change. Numerical analyses are carried out for composite laminates considering various lamination sequences (cross-ply as well as angle-ply), boundary conditions, loading conditions, span-thickness ratio, etc. The present results are compared with the existing analytical and numerical results and their agreement is observed. The effect of fiber orientation angle on bending response is analyzed to enable the optimal design of laminated composite structures under thermo-mechanical loading.</p>
3.	<p><a href="#">A review on artificial pancreas and regenerative medicine used in the management of Type 1 diabetes mellitus</a>  P Sachdeva, R Shukla, A Sahani - Journal of Medical Engineering &amp; Technology, 2022</p> <p><b>Abstract:</b> Diabetes mellitus is one of the fastest-growing lifestyle disorders in the world. While numerous regimes have been developed to manage diabetes, there continue to be high numbers of diabetes-related deaths worldwide. The review gives a brief introduction to the pathology and aetiology of the disorder, different solutions developed over time with their advantages and disadvantages, and highlights the technological components and challenges of the latest</p>

	technologies: artificial pancreas and regenerative medicine. The study is restricted to a set of high-quality publications from the last decade.
4.	<p><a href="#">Activation-Induced Surface Modulation of Biowaste-Derived Hierarchical Porous Carbon for Supercapacitors</a> P Sharma, D Singh, M Minakshi, S Quadsia, R Ahuja – ChemPlusChem, 2022</p> <p><b>Abstract:</b> Wheat straw-derived carbon from the Wheatbelt region in Western Australia was subjected to chemical activation in an electrolyte containing either acid or base treatment. The findings showed an increase in electron/hole mobility towards the interfaces due to the presence of different surface functional groups such as C-SO<sub>x</sub>-C and S=C in the carbon framework for acid activation. Likewise, the galvanostatic capacitance measured at a current density of 2 mA cm<sup>-2</sup> in a three-electrode configuration for acid-activated wheat straw exhibited 162 F g<sup>-1</sup>, while that for base-activated wheat straw exhibited 106 F g<sup>-1</sup>. An increase of 34.5% more capacitance was achieved for acid-treated wheat straw. This improvement is attributed to the synergistic effects between surface functional groups and electrolyte ions, as well as the electronic structure of the porous electrode.</p>
5.	<p><a href="#">An Analytical Approach to Locate Short Circuit Fault in a Cable Using Sweep Frequency Response Analysis</a> A Das, CC Reddy - IEEE Transactions on Industrial Electronics, 2022</p> <p><b>Abstract:</b> In this paper, analytical methods are proposed for the location of a short circuit fault in a power cable using sweep frequency response analysis (SFRA). The impedance spectroscopy is estimated using classical transmission line (TL) theory whereas the driving point impedance function (DPIF) of the cable is proposed to be constructed either by using experimental SFRA data or analytically from the knowledge of the frequency-dependent parameters, material properties, and dimensions of the cable. Finally, an analytical formula is proposed for the estimation of the location of a short-circuit fault using the location of poles and zeros of the impedance function before and after the fault. The formulae are validated using FEM software simulations as well as experimentally on a test cable.</p>
6.	<p><a href="#">An in silico model for woven bone adaptation to heavy loading conditions in murine tibia</a> A Goyal, J Prasad - Biomechanics and Modeling in Mechanobiology, 2022</p> <p><b>Abstract:</b> Existing in silico models for lamellar bone adaptation to mechanical loading are unsuitable for predicting woven bone growth. This anomaly is due to the difference in mechanobiology of the woven bone with respect to that of the lamellar bone. The present study is aimed at developing an in silico bone-adaptation model for woven bone at cellular and tissue levels. The diffusion of Ca<sup>2+</sup> ions reaching lining cells from the osteocytic network and the bone cortex in response to a mechanical loading on the cortical bone has been considered as a stimulus. The diffusion of ions within osteocytic network has been computed with a lacunar-canalicular network (LCN) in which bone cells are uniformly arranged. Strain energy density is assumed to regulate ion flow within the network when the induced normal strain is above a threshold level. If the induced strain exceeds another higher threshold level, then the strain with a power constant is additionally assumed to regulate the stimulus. The intracellular flow of Ca<sup>2+</sup> ions within the LCN has been simulated using Fick's laws of diffusion, using a finite element method. The ion diffusion from bone cortex to vesicles has been formulated as a normal strain with a power constant. The stimuli reaching the surface cells are assumed to form the new</p>

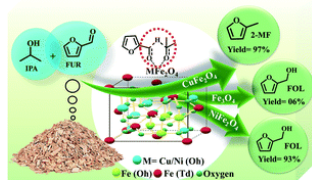
	bone. The mathematical model closely predicts woven bone growth in mouse and rat tibia for various in vivo loading conditions. This model is the first to predict woven bone growth at tissue and cellular levels in response to heavy mechanical loading.
7.	<p><a href="#">An Emergency Message and Call System for People with Epilepsy</a> RS Krishnu, R Shukla, HK Chattar, BS Paul, R Kaur, A Khokhar, G Singh, AK Sahani - Conference Record - IEEE Instrumentation and Measurement Technology Conference, 2022</p> <p><b>Abstract:</b> People with epilepsy (PWE) always worry about mishaps that can happen to them due to seizure attacks if someone is not nearby. To overcome this, we have developed a novel alert system that can help caretakers to reach patients quickly. The system consists of cloud services that record the alert signal received from the user. Emergency call is triggered through a raspberry pi - GSM module interface. A mobile application was developed to save caretaker contacts and share location details while an epileptic patient sends out alarm signals. These location details are conveyed to caretakers as google map link and address through call and message. By using cloud services and an emergency call module that can be kept anywhere with undisturbed network connectivity, the epilepsy patients with the installed application can initiate alert services and send distress messages to all caretakers with minimal effort. The average delays for calls and message received at caretaker's end from pushing the alarm signal are recorded as 13.6 and 8 seconds respectively.</p>
8.	<p><a href="#">An Unconventional Measurement Technique to Estimate Power Transfer Efficiency in Series-Series Resonant WPT System Using S-Parameters</a> A Bharadwaj, A Sharma, CC Reddy - IEEE Transactions on Instrumentation and Measurement, 2022</p> <p><b>Abstract:</b> Power transfer efficiency is a critical performance parameter for the coil design of a wireless power transfer (WPT) system. An accurate and simplistic measurement technique of power transfer efficiency will ensure the system less susceptible to the external environment with high reliability. Broadly, S-parameter-based efficiency is considered a precise measurement technique attained by the network analyzer. However, it lacks consistency in the practical scenario, the input–output ports being calibrated at <math>50 \Omega</math>. Accordingly, most of the power dissipates in the instrument's internal resistance. Therefore, this article proposes a novel S-parameter efficiency measurement technique aided by user-calibrated source and load factors. This technique's output ensures the WPT system's performance assessment even at high frequencies by S-parameters at all conditions. Besides, the proposed technique is experimentally verified and compared with various conventional techniques employed in several literary works.</p>
9.	<p><a href="#">Analysis of differential glacier behaviour in Sikkim Himalayas in view of changing climate</a> S Guha, RK Tiwari - Geocarto International, 2022</p> <p><b>Abstract:</b> The assessment of temporal changes in glacier response due to climatic change is critical from the hydrological perspective. The present study aims to identify temporal changes in glacier response using area changes, retreat, and surface elevation changes. The Friedman test and Wilcoxon signed-rank test were introduced to identify the temporal changes in the parameters mentioned above for the entire Sikkim from a sample of 28 studied glaciers. The result shows the area changes lies between 0.044–0.462, 0.143–0.351, 0.083–0.685, and 0.157–1.39%<math>y^{-1}</math> between 1988–2000, 2000–08, 2008–14 and 2014–18, respectively. Further, the magnitude of deglaciation has increased after 2014 by 73%, 76%, and 100% compared to the</p>

	<p>third, second, and first timeframe. Likewise, retreat is <math>10.82 \pm 3.53</math>, <math>19.07 \pm 4.19</math>, <math>13.32 \pm 5.59</math>, <math>23.44 \pm 5.3</math> <math>\text{my}^{-1}</math> between 1998–2000, 2000–08, 2008–14 and 2014–18, respectively in the sample glaciers. Additionally, surface elevation change shows a negative-accelerated trend in the sample glaciers from <math>0.15</math> to <math>1.92</math> <math>\text{my}^{-1}</math> to <math>0.88</math> to <math>2.52</math> <math>\text{my}^{-1}</math> between 2000–08 and 2008–18, respectively.</p>
10.	<p><a href="#">Analytical solutions for predicting seepage in a layered ditch drainage system under Dirichlet and lagging Robin boundary conditions</a>  R Sarmah, I Sonkar, SR Chavan - Hydrological Sciences Journal, 2022</p> <p><b>Abstract:</b> The present study proposed two analytical solutions for a layered ponded ditch drainage system with Dirichlet and lagging Robin boundary conditions. The flow domain is assumed to be saturated, layered, and anisotropic. The first analytical model considers flow to a ditch drainage network from a ponded field through a two-layered soil considering Dirichlet boundary condition, whereas the second model is developed considering lagging Robin condition at the ditch face and surface of the soil. The study highlights that the lagging Robin condition can better mimic the actual flow scenario as compared to the standard Robin boundary condition. A comparison study has been carried out to assess the top layer's permissible depth under which a homogeneous drainage system with Robin boundary condition can approximate a layered drainage system. Further, the residence time distributions are observed to follow power-law-like distributions with heavier tails for both single and two-layered ditch drainage systems.</p>
11.	<p><a href="#">Asymptotic analysis of an interior optimal control problem governed by Stokes equations</a>  S Garg, BC Sardar - Mathematical Methods in the Applied Sciences, 2022</p> <p><b>Abstract:</b> This article introduces an interior optimal control problem (OCP) in a two-dimensional domain with a highly oscillatory boundary governed by the stationary Stokes equations. We consider the periodic controls in the oscillating region of the domain and use the unfolding operators to characterize the optimal controls. We establish the convergences of optimal control, state, and pressure in a suitable space to the ones of the limit system in a fixed domain.</p>
12.	<p><a href="#">Automatic Double Contact Fault Detection in Outdoor Volleyball Videos</a>  P Kumari, A Kumar, M Hu, M Saini - International Conference on Computer Vision and Image Processing, 2022</p> <p><b>Abstract:</b> One of the common faults in volleyball is double contact while setting the ball for a spike. It is hard to detect this fault by the players. Even the referees sometimes find it difficult to observe. In this work, we propose an automatic double contact fault detection approach using a single camera in outdoor volleyball video. The video is first analyzed to detect and track the ball; the bounding boxes are then processed to extract a deep Spatio-temporal representation using a state-of-the-art 3D-convolution-based neural network, which is finally fed to a multilayer perceptron for classification. To the best of our knowledge, this is the first work on volleyball double-contact detection. The proposed framework achieves an average accuracy of 77.16% on 5-fold cross-validation. The framework is useful for players during training and for referees as a decision-support tool.</p>
13.	<p><a href="#">Biaxial stress and functional groups (T = O, F, and Cl) tuning the structural, mechanical, and electronic properties of monolayer molybdenum carbide</a>  K Kotmool, T Kaewmaraya, T Hussain, R Ahuja, W Luo.. - Phys. Chem. Chem. Phys., 2022</p>

	<p><b>Abstract:</b> MXenes are a family of novel two-dimensional (2D) materials attracting intensive interest because of the rich chemistry rooted from the highly diversified surface functional groups. This enables the chemical optimization suitable for versatile applications, including energy conversion and storage, sensors, and catalysis. This work reports the <i>ab initio</i> study of the crystal energetics, electronic properties, and mechanical properties, and the impacts of strain on the electronic properties of tetragonal (1T) and hexagonal (2H) phases of Mo<sub>2</sub>C as well as the surface-terminated Mo<sub>2</sub>CT<sub>2</sub> (T = O, F, and Cl). Our findings indicate that 2H-Mo<sub>2</sub>C is energetically more stabilized than the 1T counterpart, and the 1T-to-2H transition requires a substantial energy of 210 meV per atom. The presence of surface termination T atoms on Mo<sub>2</sub>C intrinsically induces variations in the atomic structure. The calculated structures were selected based on the energetic and thermodynamic stabilities (400 K). The O atom prefers to be terminated on 2H-Mo<sub>2</sub>C, whereas the Cl atom energetically stabilizes on 1T-Mo<sub>2</sub>C. Meanwhile, with certain configurations, 2H-Mo<sub>2</sub>CF<sub>2</sub> and 1T-Mo<sub>2</sub>CF<sub>2</sub> with slightly different energies could exist simultaneously. The Mo<sub>2</sub>CO<sub>2</sub> possesses the highest mechanical strength and elastic modulus (<math>\sigma_{\max} = 52</math> GPa at <math>\epsilon_b = 20\%</math> and <math>E = 507</math> GPa). The nature of the ordered centrosymmetric layer and the strong bonding between 4 d-Mo and 2 p-O of 2H-Mo<sub>2</sub>CO<sub>2</sub> are responsible for its promising mechanical properties. Interestingly, the topological properties of 2H-Mo<sub>2</sub>CO<sub>2</sub> at a wide range of strains (−10% to 12%) are reported. Moreover, 2H-Mo<sub>2</sub>CF<sub>2</sub> is metallic through the range of calculation. Meanwhile, originally semiconducting 1T-Mo<sub>2</sub>CF<sub>2</sub> and 1T-Mo<sub>2</sub>CCl<sub>2</sub> preserve their features under the ranges of the strain of −2% to 10% and −1% to 5%, respectively, beyond which they undergo the semiconductor-to-metal transitions. These findings would guide the potential applications in modern 2D straintronic devices.</p>
14.	<p><a href="#"><u>Catalytic interplay of metal ions (Cu<sup>2+</sup>, Ni<sup>2+</sup>, and Fe<sup>2+</sup>) in MFe<sub>2</sub>O<sub>4</sub> inverse spinel catalysts for enhancing the activity and selectivity during selective transfer hydrogenation of furfural into 2-methylfuran</u></a>  GS More, A Shivhare, SP Kaur, TJD Kumar, R Srivastava - <i>Catalysis Science and Technology</i>, 2022</p> <p><b>Abstract:</b> 2-Methylfuran obtained <i>via</i> the hydrogenation of furfural is an important biomass-derived liquid fuel. However, the large-scale production of 2-methylfuran from furfural requires cost-effective, active, and selective heterogeneous catalysts. Herein, we have performed experimental and DFT investigations on MFe<sub>2</sub>O<sub>4</sub> (M = Cu<sup>2+</sup>, Ni<sup>2+</sup>, and Fe<sup>2+</sup>) inverse spinel catalysts to selectively hydrogenate furfural into 2-methylfuran <i>via</i> transfer hydrogenation, and to determine the nature of active sites. CuFe<sub>2</sub>O<sub>4</sub> afforded 99.4% furfural conversion and 97.6% 2-methylfuran selectivity at 200 °C in 1.5 h. In contrast, NiFe<sub>2</sub>O<sub>4</sub> and Fe<sub>3</sub>O<sub>4</sub> catalysts afforded furfuryl alcohol as a major product. The comprehensive characterization of the catalysts revealed that the acidity of these inverse spinel catalysts originates from the Lewis acid sites. Further, the strength of Lewis acid sites and the associated catalytic activity trend directly correlate with the binding energy of Fe<sup>n+</sup> ions in MFe<sub>2</sub>O<sub>4</sub> catalysts. DFT calculations revealed the energetically favorable interactions of furfural and furfural alcohol with the Fe<sup>3+</sup> sites of Fe<sub>3</sub>O<sub>4</sub> and Fe sites (most likely Fe<sup>3+</sup>) of CuFe<sub>2</sub>O<sub>4</sub> and NiFe<sub>2</sub>O<sub>4</sub> catalysts, whereas Cu<sup>2+</sup> and Ni<sup>2+</sup> sites present in CuFe<sub>2</sub>O<sub>4</sub> and NiFe<sub>2</sub>O<sub>4</sub> catalysts have stronger interactions with the isopropanol molecule. Hence, it is proposed that the Fe<sup>3+</sup> sites present in CuFe<sub>2</sub>O<sub>4</sub> are the active Lewis acid centers to selectively convert furfural into 2-methylfuran <i>via</i> transfer hydrogenation. Literature reports on the metal oxide catalyzed transfer hydrogenation of furfural into 2-methylfuran are rare. The</p>



present findings on the elucidation of the active sites of cost-effective, recyclable mixed metal oxide catalysts for the selective transfer hydrogenation of furfural into 2-methylfuran using isopropanol are attractive from the green chemistry perspective, and therefore extremely important for the academic catalysis community and to industrialists.



15. [Channel Difference Based Regeneration Architecture for Fake Colorized Image Detection](#)  
 SS Phutke, S Murala - International Conference on Computer Vision and Image Processing, 2022

**Abstract:** Selling of counterfeit/fraud goods like publishing the fake images of the products is increasing now a days due to advancement of multimedia technology for image editing applications. This work aims to detect the fake colorized images with a novel observation of channel difference maps. Here, we propose a novel deep channel difference network for fake colorized image detection/classification. Initially, an effective channel difference map (CDM) based auto-encoder is proposed for image regeneration. Here, to get distinguishing edge and color information between real and fake colorized images, CDM is proposed. After effective regeneration, the abstract version of learned features can be used for classification. Thus, we have proposed the transfer learning based network for fake colorized image detection (FCID) with learned encoder features of regeneration network. To the best of our knowledge, this is the first work with CDM based auto-encoder for FCID. The performance of the proposed network is tested on benchmark datasets and compared with the existing state-of-the-art methods for FCID in terms of half total error rate (HTER). The experimental results demonstrate that the proposed network is superior than the state-of-the-art approaches for FCID.

16. [Chapter 9 Rheology of Dilute Inertial Suspensions](#)  
 G Subramanian, NK Marath - Recent Advances in Rheology, 2022


**Abstract:** In inertial suspensions, inertia becomes important on the scale of the disperse particulate phase (the ‘micro-scale’). From the rheological standpoint, the interest is in suspensions of neutrally buoyant particles, with micro-scale inertial effects characterized by the particle Reynolds number. Dilute inertial suspensions differ fundamentally from their Stokesian counterparts, in possessing a non-Newtonian rheology and a finite microstructural relaxation time, even in the absence of interparticle interactions. We discuss the role of micro-scale inertia for dilute suspensions of both spherical and anisotropic particles. The discussion on inertial suspensions is preceded by one on Stokesian suspensions, the emphasis being on the rheological indeterminacy arising from either an indeterminate pair-distribution function (spherical particles), or an indeterminate single-particle orientation distribution (spheroidal particles). The effect of inertia is accordingly classified into: (1) a ‘direct effect’ where inertial contributions to rheological properties explicitly involve the particle Reynolds number, and become vanishingly small when the Reynolds number goes to zero; and (2) an ‘indirect effect’ where inertia determines the leading order viscosity, even for vanishingly small Reynolds numbers, due to the Stokesian indeterminacy. As part of the indirect effect, we discuss the tumbling-spinning

	<p>transition for inertial suspensions of thin oblate spheroids, and the role of stochastic orientation fluctuations in leading to a transition from a shear-thickening to a shearthinning rheology, with changing aspect ratio, for sufficiently long times; and hysteretic behavior for shorter times. While the emphasis is mainly on theoretical calculations for small particle Reynolds numbers, where applicable we discuss simulations that provide insight into inertial effects at finite particle Reynolds number. Although micro-scale inertia is predicted to have profound rheological consequences, measurements of the same pose problems. Traditional rheometric devices are prone to instabilities and secondary flows arising from macro-scale inertia, and we therefore end with a discussion of recent suspension-transition experiments (a non-rheometric setting), that would allow for an inference of the underlying inertial rheology.</p>
17.	<p><a href="#">Collective excitations in cigar-shaped spin-orbit-coupled spin-1 Bose-Einstein condensates</a> Rajat, A Roy, S Gautam – Physical Review A, 2022</p> <p><b>Abstract:</b> We study theoretically the collective excitations of a spin-orbit-coupled spin-1 Bose-Einstein condensate with antiferromagnetic spin-exchange interactions in a cigar-shaped trapping potential at zero and finite temperatures using the Hartree-Fock-Bogoliubov theory with Popov approximation. The collective modes at zero temperature are corroborated by real-Time evolution of the ground state subjected to a perturbation suitable to excite a density or a spin mode. We also calculate a few low-lying modes analytically and find very good agreement with the numerical results. We confirm the presence of excitations belonging to two broad categories, namely, density and spin excitations, based on the calculation of dispersion. The degeneracy between a pair of spin modes is broken by the spin-orbit coupling. At finite temperature, spin and density excitations show qualitatively different behavior as a function of temperature.</p>
18.	<p><a href="#">Commissioning the FAst TIMing array (FATIMA) at FAIR Phase-0: Half-lives of excited states in the N=50 isotones <sup>96</sup>Pd and <sup>94</sup>Ru</a> S Jazrawi, A Yaneva, M Polettini, A Sharma.. - Radiation Physics and Chemistry, 2022</p> <p><b>Abstract:</b> This paper reports results of the first experiment of the DESPEC Phase-0 campaign at GSI, which focused on the study of neutron-deficient nuclei approaching <sup>100</sup>Sn. These data provide the first extended commissioning experiment for the DESPEC collaboration within NuSTAR. We present results on electromagnetic transition rates associated with the decays from excited states populated following the formation of <math>I^\pi = 8^+</math> proton ‘seniority-isomer’ states in the N = 50 isotones <sup>94</sup>Ru and <sup>96</sup>Pd. Direct half-life measurements via <math>\gamma</math>-<math>\gamma</math> coincidences using the FATIMA detector array consisting of 36 LaBr<sub>3</sub>(Ce) scintillators have determined the reduced matrix elements associated with decays between low-lying states in these semi-magic nuclei. The extracted half-lives for yrast <math>I^\pi = 6^+</math> and <math>4^+</math> states in <sup>96</sup>Pd and the <math>6^+</math> state in <sup>94</sup>Ru are consistent with the published, highest-precision values for these nuclei.</p>
19.	<p><a href="#">Concept of optimum basin thickness in heat exchanger–assisted solar stills</a> S Verma, R Das - Environmental Science and Pollution Research, 2022</p> <p><b>Abstract:</b> It is suggested by many works on solar stills that water thickness should be kept as low as possible to reduce its thermal inertia and obtain best results. However, when external heat addition is employed by an internal exchanger, the amount of heat addition is also affected by the still water thickness, and so, the above-mentioned finding could be proved incorrect. In this context, here, the performance of a solitary basin solar still aided by external heat addition has been revisited. At first, an expression for the maximum possible effectiveness of the above-</p>

	<p>mentioned exchanger is derived. Based on this, improved closed form solutions for the still water temperature and still productivity have been obtained using integrating factor method. It is shown that the closed form solutions presented here are mathematically superior to other analytical solutions available in the literature on the topic, in the sense that the present ones are strictly analytical, while all others use an iterative algorithm to solve the pertinent differential equation. Contrary to the available studies on solar stills which suggest keeping the water thickness to its minimum possible value, the present results reveal an optimum thickness of the same to maximize the system productivity. Using the optimized still water thickness, about 35 and 41% enhancement in the daily and annual productivity respectively can be acquired with respect to the thickness suggested by the available literature. The optimum value stems from a trade-off between the efficiency of external heat addition and the thermal inertia of the water mass. This work therefore suggests the thickness of water mass in heat exchanger-based solar stills to be designed at an optimum value for best results, and also provides useful improved expressions for performance assessment of such stills.</p>
20.	<p><a href="#">Critical Review on the Utilization of Robotic-system Point-to-point-based Position Actuators and Laser Sensors with Artificial Intelligence Mediator in an Archetypal Mechatronics Network for Medical Dermatology Applications</a>  S Sharma, H Garg, J Singh, J Singh, N Gautam.. - International Journal of Health Sciences, 2022</p> <p><b>Abstract:</b> In this article, a comprehensive overview of the classic designing of mechatronics-based robotics components like sensors and effectors in a network to solve the problems related to the medical skin of the human body with the help of an Artificial Intelligence has been carried out. Area-based artificial agent is the easiest way to deal with the skin-related diseases. In this artificial agent, we are having autonomy and flexibility to work on the area.</p>
21.	<p><a href="#">Decay studies in the <math>A \sim 225</math> Po-Fr region from the DESPEC campaign at GSI in 2021</a>  M Poletini, J Pellumaj, G Benzoni, A Sharma.. - Nuovo Cimento della Societa Italiana di Fisica C, 2022</p> <p><b>Abstract:</b> The HISPEC-DESPEC collaboration aims at investigating the structure of exotic nuclei formed in fragmentation reactions with decay spectroscopy measurements, as part of the FAIR Phase-0 campaign at GSI. This paper reports on first results of an experiment performed in spring 2021, with a focus on <math>\beta</math>-decay studies in the Po-Fr nuclei in the <math>220 &lt; A &lt; 230</math> island of octupole deformation exploiting the DESPEC setup. Ion-beta correlations and fast-timing techniques are being employed, giving an insight into this difficult-to-reach region.</p>
22.	<p><a href="#">Defect Detection Using Correlation Approach for Frequency Modulated Thermal Wave Imaging</a>  A Rani, V Arora, Ramachandra SK, R Mulaveesala - Smart Innovation, Systems and Technologies, 2022</p> <p><b>Abstract:</b> Defect detectability of structures and components is one of the significant parameters for proper functioning of industries. Active thermography is a safe and reliable technique for non-destructive testing and evaluation (NDT&amp;E) of these materials during in-service applications. This paper investigates the defect resolvability in a carbon fiber reinforced polymer (CFRP) sample using frequency modulated thermal wave imaging (FMTWI) technique. FMTWI performance has been examined using correlation-based pulse compression (PC) approach and compared with the conventional data processing approaches. Results shows the high sensitivity and resolution to resolve deeper defects of varying depths and diameters in CFRP sample using</p>



	correlation approach.
23.	<p><a href="#">Detection and detoxification of imidacloprid in food samples through ionic liquid-stabilized CuNi alloy nanoparticle-decorated multiwall carbon nanotubes</a> M Kumar, N Kaur, N Singh - Environmental Science: Nano, 2022</p> <p><b>Abstract:</b> The development of resourceful catalysts with effective quantification as well as the detoxification of insecticides is a major challenge in terms of food safety and sustainable agriculture. The present study reports the development of ionic liquid-stabilized CuNi alloy nanoparticle-decorated MWCNTs (CuNi/IL@MWCNTs) via a simple reduction method and the characterization techniques confirm the morphology, size and oxidation state of CuNi/IL@MWCNTs. Furthermore, the CuNi/IL@MWCNTs/glass carbon electrode (GCE) showed selectivity and excellent electrocatalytic activity towards imidacloprid (IMD), resulting in exceedingly low limit of detection (11 nM), good stability, and wide linear range (0.0125-240 <math>\mu</math>M) for the detection of imidacloprid. Interestingly, CuNi/IL@MWCNTs also show excellent recovery results (97.4-101.2%) in spiked corn and rice samples. In addition to the quantification of IMD, the CuNi/IL@MWCNTs achieved almost complete degradation (up to 99.6%) behavior to detoxify the IMD in an aqueous system in 100 s with good reusability. Confidently, the proposed study can provide a functional material for the sensitive detection and quick detoxification of low concentration IMD in food samples in developing and remote areas.</p>
24.	<p><a href="#">Diffusion of multi-principal elements through stable Cr<sub>2</sub>O<sub>3</sub> and Al<sub>2</sub>O<sub>3</sub> scales</a> I Roy, PK Ray, G Balasubramanian – Materialia, 2022</p> <p><b>Abstract:</b> Understanding the oxidation mechanisms in multi-principal elements and high-entropy alloys (HEAs) is critical for their potential applications in high-temperature oxidative environments. In addition to the compositional complexity, the counter-diffusion of cations and anions through the oxide contributes to the growth of the oxide scales in these materials. We examine the cationic and anionic diffusion through the stable chromium and aluminum oxides that form in a model HEA using atomistic simulations. In accord with experiments, we find that the tracer cations diffuse faster than the native cations through the oxide scales at high temperature (1000 K to 2000 K) and the dynamics are directly correlated to the respective migration energies of the diffusion pathways. The oxide scale growth is strongly influenced by the presence of tracer/impurity elements in alumina forming alloys relative to those that predominantly form chromia. A geometric analysis of the vacancy-induced diffusion paths for the cation migration relative to the location of the oxygen atoms reveals the influence of the latter on the preferential diffusion pathway, resulting in anisotropy. The predictions offer insights on the diffusion characteristics in the oxide scales formed in HEAs and aid in our understanding of the oxide growth kinetics.</p>
25.	<p><a href="#">Direct oxidation of cyclohexane to adipic acid in air over Co<sub>3</sub>O<sub>4</sub>@ZrO<sub>2</sub> nanostructured catalyst</a> S Bhandari, R Khatun, MK Poddar, AC Kothari, R Bal - Molecular Catalysis, 2022</p> <p><b>Abstract:</b> Despite the vast industrial importance of adipic acid (AA), developing sustainable and selective catalysts for the oxidation of cyclohexane using air as an oxidant is a longstanding challenge for researchers. We have synthesized a Co<sub>3</sub>O<sub>4</sub>@ZrO<sub>2</sub> nanostructured catalyst and found that it converts cyclohexane to AA directly in air without adding any additional reagent. Under mild, environmentally friendly, solvent-free conditions and without any initiators, the catalyst showed a conversion of ~40% with a selectivity of ~43% towards adipic acid. NH<sub>3</sub>-</p>

	<p>TPD analysis confirmed the presence of acidic sites on <math>\text{Co}_3\text{O}_4@\text{ZrO}_2</math>. According to the findings, loading <math>\text{Co}_3\text{O}_4</math> in the <math>\text{ZrO}_2</math> matrix generated a considerable increase in acidity (1.08 mmol/g), and the trend of different loading of cobalt followed the order: <math>5.4\text{Co}_3\text{O}_4@\text{ZrO}_2 &gt; 3.2\text{Co}_3\text{O}_4@\text{ZrO}_2 &gt; 2.5\text{Co}_3\text{O}_4@\text{ZrO}_2 &gt; 1.6\text{Co}_3\text{O}_4@\text{ZrO}_2</math>. The catalyst was thoroughly characterized by XRD, BET, HR-TEM, SEM, <math>\text{H}_2</math>-TPR, XPS, <math>\text{NH}_3</math>-TPD, Pyridine-IR, TGA, Raman, ICP-AES, UV-Visible and EPR spectroscopy. The recyclability and leaching test confirmed the true heterogeneous nature of the catalyst as there was no significant loss of catalytic activity even after 5 cycles.</p> <p><b>Graphical Abstract:</b></p> 
26.	<p><a href="#">Distilling physical origins of hardness in multi-principal element alloys directly from ensemble neural network models</a>  D Beniwal, P Singh, S Gupta, MJ Kramer, DD Johnson, PK Ray - npj Computational Materials, 2022</p> <p><b>Abstract:</b> Despite a plethora of data being generated on the mechanical behavior of multi-principal element alloys, a systematic assessment remains inaccessible via Edisonian approaches. We approach this challenge by considering the specific case of alloy hardness, and present a machine-learning framework that captures the essential physical features contributing to hardness and allows high-throughput exploration of multi-dimensional compositional space. The model, tested on diverse datasets, was used to explore and successfully predict hardness in <math>\text{Al}_x\text{Ti}_y(\text{CrFeNi})_{1-x-y}</math>, <math>\text{Hf}_x\text{Co}_y(\text{CrFeNi})_{1-x-y}</math> and <math>\text{Al}_x(\text{TiZrHf})_{1-x}</math> systems supported by data from density-functional theory predicted phase stability and ordering behavior. The experimental validation of hardness was done on <math>\text{TiZrHfAl}_x</math>. The selected systems pose diverse challenges due to the presence of ordering and clustering pairs, as well as vacancy-stabilized novel structures. We also present a detailed model analysis that integrates local partial-dependencies with a compositional-stimulus and model-response study to derive material-specific insights from the decision-making process.</p>
27.	<p><a href="#">Effects of fluid shear-thinning and yield stress on free convection in concentric and eccentric cylindrical annuli</a>  G Mishra, P Mishra, RP Chhabra - International Journal of Thermal Sciences, 2022</p> <p><b>Abstract:</b> Laminar free convection in yield-pseudoplastic fluids (the Herschel-Bulkley model) for concentric and eccentric cylindrical annuli has been studied numerically. The combined effects of shear-thinning viscosity and yield stress on the heat transfer characteristics have been examined for the following ranges of parameters: Rayleigh number, <math>\text{Ra}</math> (<math>10^3</math> to <math>10^6</math>), Oldroyd number, <math>\text{Od}</math> (0 to <math>\text{Od}_{\text{max}}</math>), power-law index, <math>n</math> (0.2–1), Prandtl number, <math>\text{Pr}</math> (10–100), eccentricity, <math>\varepsilon</math> (0–1.18) and angular position of the inner cylinder, <math>\phi</math> (<math>0^\circ</math> to <math>180^\circ</math>). The results are interpreted in terms of the yield surfaces, fraction of yielded fluid, streamlines, isotherms, local Nusselt number and average Nusselt number. Overall, the eccentric positioning of the heated cylinder along the vertical centreline fosters convective transport with reference to that for the case of the</p>

	<p>concentric annulus. It is possible to achieve augmentation of up to 30% in heat transfer for the case of <math>\varepsilon = 1.18</math>, <math>\phi = 0^\circ</math> with respect to the concentric case at <math>Ra = 10^5</math>, <math>Pr = 10</math>. This is ascribed to the greater fraction of the annular area occupied by the yielded fluid-like regions. Conversely, horizontal shifting of the inner cylinder to an off-centre position has an adverse effect on heat transfer. Limited transient simulations have also been run to identify the conditions for the loss of steady flow behaviour. A predictive correlation has been developed for the average Nusselt number for its estimation in new applications.</p>
28.	<p><a href="#">Effect of micelle breaking rate and wall slip on unsteady motion past a sphere translating steadily in wormlike micellar solutions</a>  S Sasmal - <i>Physics of Fluids</i>, 2022</p> <p><b>Abstract:</b> Many prior experimental studies have found the existence of an unsteady or fluctuating flow field around a solid sphere when falling in wormlike micellar solutions. Based on the two-species Vasquez–Cook–McKinley constitutive model for micelles, a recent numerical study shows that the breakage of long micelles downstream of the translating sphere causes this unsteady motion [C. Sasmal, “Unsteady motion past a sphere translating steadily in wormlike micellar solutions: A numerical analysis,” <i>J. Fluid Mech.</i> 912, A52, (2021)]. This numerical study further shows that the micelle breakage rate and wall slip can strongly influence this phenomenon. In particular, we find that the onset of this unsteady motion is delayed to higher values of the Weissenberg number as the micelle breakage rate decreases, or in other words, micelles become hard to break. Additionally, we observe that at some values of the micelle breakage rate, again, a transition in the flow field from unsteady to steady occurs at high Weissenberg numbers. Therefore, there is a window of the Weissenberg number present to observe this unsteady motion past the translating sphere. On the other hand, we show that the presence of wall slip on the sphere surface suppresses this unsteady motion past the translating sphere, and a probable explanation is also provided for the same.</p>
29.	<p><a href="#">Effect of micelle breakage rate on flows of wormlike micellar solutions through pore throats</a>  MB Khan, C Sasmal - <i>Journal of Non-Newtonian Fluid Mechanics</i>, 2022</p> <p><b>Abstract:</b> Many practical applications such as enhanced oil recovery or groundwater remediation encounter the flow of viscoelastic wormlike micellar solutions (WLMs) through porous media. A model porous media, consisting of a microchannel with pore throats present in it, is often used to understand the flow dynamics of these complex fluids. This study performs an extensive numerical investigation to understand the complex flow behaviour of these WLMs through such a model porous media based on the two-species Vasquez–Cook–McKinley (VCM) model for micelles. Within the present range of conditions encompassed in this study, we find the existence of an elastic instability once the Weissenberg number exceeds a critical value as it was seen in many prior experimental and numerical studies dealing with polymer solutions. However, for the present case of a WLM solution, we observe that the micelle breakage rate greatly influences these instabilities. In particular, we observe that the intensity of this instability (characterized by the fluctuating flow field) increases with the Weissenberg number up to a critical value of it. Beyond that, it starts to decrease on further increment in the Weissenberg number. This is in contrast to that seen in a polymer solution where the flow field gradually transits to a more chaotic and turbulent-like state (the so-called elastic turbulence state) as the Weissenberg number gradually increases. Furthermore, we notice that the flow dynamics of these WLM solutions strongly depend on the type (symmetric or asymmetric), number, and</p>

	<p>spacing between two consecutive pore throats. Additionally, an extensive discussion on the pressure drop and relative viscosity is presented in the present study. Although this study is carried out for a model porous system, we hope it will facilitate a better understanding of the flow behaviour of wormlike micellar solutions in an actual porous media.</p>
30.	<p><a href="#"><u>Effect of multi-walled carbon nanotubes on DC electrical conductivity and acetone vapour sensing properties of polypyrrole</u></a>  A Husain, DK Mahajan - Carbon Trends, 2022</p> <p><b>Abstract:</b> Polypyrrole (PPy) and polypyrrole/multi-walled carbon nanotubes nanocomposite (PPy/MWCNTs) were synthesized and characterized by Fourier transform infrared spectroscopy (FT-IR), X-ray diffraction (XRD), scanning electron microscopy (SEM), transmittance electron microscopy (TEM) and thermogravimetric analysis (TGA). PPy and PPy/MWCNTs were converted into pellets which were used in conductivity and acetone sensing experiments. The initial electrical conductivity of PPy increased from <math>0.16 \text{ Scm}^{-1}</math> to <math>2.27 \text{ Scm}^{-1}</math> by loading of MWCNTs into PPy matrix. At the same time, PPy/MWCNTs showed excellent conductivity retention properties as compared to PPy under both the isothermal and cyclic ageing conditions. A comparative acetone vapour sensing studies were carried out on PPy and PPy/MWCNTs sensors at different acetone concentration, i.e., 0.5, 0.4, 0.3, 0.2, 0.1, 0.05, 0.04, 0.03, 0.02 and 0.01 vol%. The PPy/MWCNTs sensor offered much-improved acetone vapour sensing performance as compared to PPy in terms of sensing response, reversibility and long term stability. PPy/MWCNTs sensor exhibited 2.44, 2.82, 3.06, 3.28, 3.88, 5.0, 5.42, 6.02, 6.08 and 7.44 times greater% sensing response than PPy sensor at 0.5, 0.4, 0.3, 0.2, 0.1, 0.05, 0.04, 0.03, 0.02 and 0.01 vol% acetone concentration, respectively.</p>
31.	<p><a href="#"><u>Effects of intake charge temperature and relative air-fuel ratio on the deterministic characteristics of cyclic combustion dynamics of a HCCI engine</u></a>  A Singh, RK Maurya - International Journal of Engine Research, 2022</p> <p><b>Abstract:</b> Homogenous charge compression ignition (HCCI) combustion can significantly reduce automotive pollution and increase the thermal efficiency of the engine. However, combustion phasing control is a major challenge in HCCI engines due to severe cyclic combustion variations. This study investigates the cyclic combustion dynamics of the HCCI engine using nonlinear dynamic methods such as return maps, recurrence plots (RPs), and recurrence quantitative analysis (RQA). Combustion stability and cyclic variations of HCCI combustion parameters were investigated on a modified four-stroke diesel engine. The experiments were conducted by varying relative air-fuel ratios ((Formula presented.)) and intake air temperatures ((Formula presented.)) at two engine speeds. In-cylinder pressure data of 2000 consecutive engine combustion cycles is logged for each test condition. In this study, deterministic characteristics of combustion phasing (<math>CA_{50}</math>) and crank angle position of maximum cylinder pressure ((Formula presented.)) are investigated and compared by employing nonlinear dynamical methods. Return maps revealed that ((Formula presented.)) is having distinct and more frequently observed deterministic characteristics in comparison to <math>CA_{50}</math>. Patterns in RPs showed a more persistent and sudden change in the combustion dynamics at higher engine speeds. Recurrence plot-based analysis found the existence of deterministic features in the combustion dynamics irrespective of the operating conditions. It was found using RQA parameters that the deterministic nature becomes stronger with a decrease in ((Formula presented.)) and any deviation in intermediate values of ((Formula presented.)). Additionally, RQA measures advocate that</p>

	<p>CA<sub>50</sub> has more deterministic characteristics at higher engine speed while (Formula presented.) at lower engine speed. Strong coupling and synchronization between (Formula presented.) and CA<sub>50</sub> is indicated by cross-recurrence plots and CPR index when engine operated with a comparatively richer mixture.</p>
32.	<p><a href="#">Enhancing process competency by forced cooling in laser bending process</a> R Yadav, DK Goyal, R Kant - Journal of Thermal Stresses, 2022</p> <p><b>Abstract:</b> Laser bending utilizes laser-induced thermal distortion to bend the sheet metal. This process is advantageous for job and batch productions but not suitable for mass production due to small bend angle per scan. This study aims to increase the bend angle per scan by applying forced cooling at the surface opposite to the laser scan. A 3-D numerical model is developed for laser bending process to analyze the effect of forced cooling on bend angle and edge effect. Results show that the bend angle can be significantly increased by applying forced cooling on the surface opposite the laser scan. However, the application of forced cooling is found to be effective only at high line energy, but it affects adversely at low line energy. Results also show that the edge effect is increased by the application of forced cooling at high line energy; however, it is marginally affected at low line energy.</p>
33.	<p><a href="#">Enhancing Corrosion Performance of Cold-Sprayed Titanium/Baghdadite (Ti/BAG) Bio-Composite Coatings via Laser Treatment</a> A Kumar, DK Goyal, R Kant, H Singh - Progress in Materials Coating for Sustainable and Emerging Applications, 2022</p> <p><b>Abstract:</b> This study aims to enhance the corrosion performance of cold-sprayed titanium/baghdadite (Ti/BAG) bio-composite coatings. Laser post processing was performed to reduce porosity and improve mechanical properties. The process parameters for laser treatment of cold-sprayed coatings were verified experimentally using scanning electron microscopy (SEM) and a thermal imaging camera. The laser-treated coatings are analyzed with SEM, energy-dispersive spectroscopy (EDS), ImageJ software, and X-ray diffraction (XRD). Furthermore, electrochemical analysis of the laser-treated and as-sprayed coatings was conducted in Ringer's solution. The results of this study revealed that laser treatment helps significantly in enhancing resistance to corrosion for Ti/BAG composite coatings in a Ringer's solution. The reduction in porosity and surface roughness is ascribed as the reason for their superior performance relative to as-sprayed coatings.</p>
34.	<p><a href="#">Environmentally conscious biomedical implant manufacturing method</a> GP Singh Sodhi, V Bhakar, G Singh, H Singh, PM Pandey, S Pan - Proceedings of the Institution of Mechanical Engineers, Part E: Journal of Process Mechanical Engineering, 2022</p> <p><b>Abstract:</b> The significant advantage of using magnesium as a surgical implant is its ability to biodegrade in situ, eliminating the requirement for implant removal surgery. However, investigating biomedical implant fabrication processes required the study analyses from the perspective of the process plan and environmental impact for better sustainable solutions. In the present study, magnesium and hydroxyapatite-based composite material have been selected for fabricating the bio-medical implant. The real-time data has been observed in the production processes. The environmental impacts of the produced bio-implant material are compared with those of the bio-implant produced using friction-stir processing and laser-based powder metallurgy. It is observed from the analysis that conventional methods can be utilized for making</p>

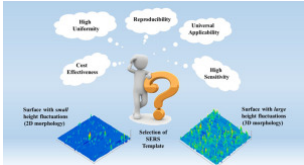


	<p>bio-medical implants cost-effectively after careful modifications in the process sequence and parameters. The environmental impact analysis provided a detailed visualization of major hotspots and supported effective decision-making toward improving the production process. At the same time, the comparative analysis provides a clear picture of the hotspots in the bio-implant production processes. The study compared the environmental impact of two bio-implant production processes and provided valuable insights to reduce overall cost and improve environmental impact across the supply chain. A bio-implant prototype has been made with a cheaper alternative to additive manufacturing.</p>
35.	<p><a href="#">Epileptic Seizure Detection Using Continuous Wavelet Transform and Deep Neural Networks</a>  R Shukla, B Kumar, G Gaurav, G Singh, AK Sahani - Lecture Notes in Electrical Engineering, 2022</p> <p><b>Abstract:</b> Seizure event detection by manually analyzing electroencephalogram (EEG) data is a routine process in epilepsy units done by trained professionals. Misdiagnosis of epileptic seizures is a common problem. Therefore, an automatic seizure detection algorithm can help neurologists in diagnosing epilepsy correctly in lesser time with higher accuracy. In this paper, we have proposed an automated seizure detection algorithm based on continuous wavelet transform (CWT) and convolutional neural networks (CNNs). Seizure and non-seizure events are classified from the University of Bonn Germany dataset. To train the Deep learning-based classifier efficiently, the amount of data is increased using a data augmentation technique. After that, the data is window segmented and continuous wavelet transform (CWT) is employed on these segments to get a scalogram plot. The image of the scalogram plot is used in training the CNN model for seizure classification. Effect of different window sizes (1 s, 2 s, and 3 s) on classification accuracy is analyzed, and 3 s window segments have shown best classification result on original and augmented data.</p>
36.	<p><a href="#">Experimentally Validated Analytical Modelling of the Laser Bending of Low Carbon Steel Sheets</a>  R Nair, R Kant, R Yadav, H Gurung - Lasers in Engineering, 2022</p> <p><b>Abstract:</b> Laser bending is used to induce precise bend angle in sheets and foils by controlled laser irradiations. In this paper an analytical model is developed to set up a relationship between bend angle and process parameters in terms of laser power and scan speed during laser sheet bending. The proposed model estimates the bend angle considering laser parameters and thermo-mechanical properties of the workpiece material. The analytical model is validated by conducting experiments on low carbon steel, and the results showed that the developed analytical model is in good agreement with the experimental results. The average absolute error between experimental and analytical bend angle is about 9.51%.</p>
37.	<p><a href="#">Exploring the dependence between discharge indices and catchment descriptors for suspended sediment load in Indian Rivers</a>  S Maheshwari, SR Chavan - ISH Journal of Hydraulic Engineering, 2022</p> <p><b>Abstract:</b> In this paper, we have explored the dependence of discharge indices (and their return period) on various catchment descriptors, such as average slope, basin relief, drainage area, maximum elevation, and mean elevation. Discharge indices, viz., effective discharge, functional-equivalent discharge, and fraction-load discharge, are considered in this study. These indices characterize long-term sediment transport through stream networks and are generally adopted as</p>

	<p>design flows for restoration of streams and in geomorphic, as well as in eco-hydrologic studies. These indices (and their return period) were determined based on a continuous probability distribution (e.g. log-normal and Gamma)-based Magnitude-Frequency Analysis approach. These indices and their return period were found to have a negative correlation with all these catchment descriptors except the drainage area. This is because there is a reduction in the magnitude of discharge indices with the rise in average slope, basin relief, maximum elevation, and mean elevation, which indicates that a lesser magnitude of flows/discharges is effective in carrying a considerable amount of sediments over time as the transport of sediments is assisted by high slopes of upstream catchments, viz., headwater catchments. These correlated descriptors can be useful in the determination of indices (and their return period) for ungauged catchments.</p>
38.	<p><a href="#">Exploring the Impact of Parametric Variability on Eye Diagram of On-Chip Multi-walled Carbon Nanotube Interconnects using Fast Machine Learning Techniques</a>  K Dimple, S Guglani, R Kumar, S Roy, BK Kaushik, S Kushwaha, R Sharma - 2022 IEEE 72nd Electronic Components and Technology Conference (ECTC), 2022</p> <p><b>Abstract:</b> In this paper, an artificial neural network (ANN) based metamodel is developed for estimating the eye diagram characteristics of on-chip multi-walled carbon nanotube (MWCNT) interconnect networks subject to parametric variability. The proposed ANN metamodel is trained using a prior knowledge input with source difference (PKID) formulation. In this PKID formulation, the eye diagram characteristics predicted by the compact but approximate equivalent single conductor (ESC) representation of the MWCNT conductors is used as prior knowledge to accelerate the learning of the ANN. Consequently, the proposed ANN metamodel can be trained at far smaller computational time costs than conventional ANN metamodels and existing multi-fidelity approaches without any discernable loss in accuracy.</p>
39.	<p><a href="#">Exploring the Role of Adversarial Attacks in Image Anti-forensics</a>  KG Sharma, G Singh, P Goyal - International Conference on Computer Vision and Image Processing, 2022</p> <p><b>Abstract:</b> Deep learning (DL) has grown significantly in the field of image forensics. A lot of research has been going on to develop deep learning based image manipulation detection techniques. On the contrary, researchers are also challenging the robustness of these DL-based image forensic techniques by developing efficient anti-forensic schemes. This paper reveals the role of adversarial attacks in image anti-forensics with better human imperceptibility against recent general-purpose image forensic techniques. We propose an image anti-forensic framework by using recent adversarial attacks, i.e., Fast Gradient Sign Method (FGSM), Carlini and Wagner (C &amp;W), and Projected Gradient Descent (PGD). Firstly, we have trained recent image forensic models on the BOSSBase dataset. Then, we generate adversarial noise by using the gradient of these image forensic models corresponding to each adversarial attack. Afterward, the obtained noise is added to the input image, resulting in the adversarial image corresponding to the particular attack. These adversarial images are generated by using the BOSSBase dataset and tested on the recent image forensic models. The experimental results show that the performance of the recent forensic models has decreased rapidly in the range from 50–75% against the different adversarial attacks, i.e., FGSM, C &amp;W, and PGD. Furthermore, the high human imperceptibility of generated adversarial images is confirmed from the PSNR values.</p>
40.	<p><a href="#">Fiction and Facts about BCG Imparting Trained Immunity against COVID-19</a>  G Kaur, S Singh, S Nanda, MA Zafar, JA Malik, MU Arshi, T Lamba, JN Agrewala – Vaccines,</p>

	<p>2022</p> <p><b>Abstract:</b> The Bacille Calmette-Guérin or BCG vaccine, the only vaccine available against Mycobacterium tuberculosis can induce a marked Th1 polarization of T-cells, characterized by the antigenspecific secretion of IFN-<math>\gamma</math> and enhanced antiviral response. A number of studies have supported the concept of protection by non-specific boosting of immunity by BCG and other microbes. BCG is a well-known example of a trained immunity inducer since it imparts ‘non-specific heterologous’ immunity against severe acute respiratory syndrome coronavirus 2 (SARS-CoV-2), the virus responsible for the recent pandemic. SARS-CoV-2 continues to inflict an unabated surge in morbidity and mortality around the world. There is an urgent need to devise and develop alternate strategies to bolster host immunity against the coronavirus disease of 2019 (COVID-19) and its continuously emerging variants. Several vaccines have been developed recently against COVID-19, but the data on their protective efficacy remains doubtful. Therefore, urgent strategies are required to enhance system immunity to adequately defend against newly emerging infections. The concept of trained immunity may play a cardinal role in protection against COVID-19. The ability of trained immunitybased vaccines is to promote heterologous immune responses beyond their specific antigens, which may notably help in defending against an emergency situation such as COVID-19 when the protective ability of vaccines is suspicious. A growing body of evidence points towards the beneficial nonspecific boosting of immune responses by BCG or other microbes, which may protect against COVID-19. Clinical trials are underway to consider the efficacy of BCG vaccination against SARSCoV-2 on healthcare workers and the elderly population. In this review, we will discuss the role of BCG in eliciting trained immunity and the possible limitations and challenges in controlling COVID-19 and future pandemics.</p>
41.	<p><a href="#">Finite element simulation of multilayer model to simulate fine needle insertion mechanism into iliac crest for bone marrow biopsy</a>  R Nadda, R Repaka, AK Sahani - Computer Methods in Biomechanics and and Biomedical Engineering, 2022</p> <p><b>Abstract:</b> The main aim of this work is to<sup>1</sup> use a finite element technique (FEM) to gain understanding about the bone marrow biopsy (BMB) needle insertion process and needle-tissue interactions in the human iliac crest. A multi-layer iliac crest model consists of stratum corneum, dermis, epidermis, hypodermis, cortical, and cancellous bone has been established. This paper proposes a FE model that examines all phases of tissue deformation, including puncture, cutting, needle-tissue interaction, and various stress-strain values for BMB needle during interaction. The results explain the needle-tissue interface and show the potential of this technique to estimate bone damage and tissue deformation for multiple needle dimensions, coefficient of friction, and penetration speeds. The insertion and extraction force of conical-shaped needles in the multi-layered iliac crest model decreased by 18.92% and 37.5%, respectively, as the needle diameter reduced from 11 G to 20 G. It has also been found that the significant insertion motion raises the deformation of the tissue due to the augmented frictional forces but reduces the strain perpendicular to the penetration direction closer to the needle tip. The simulation outcomes are helpful for the optimal design of fine biopsy needles used to perform the bone marrow biopsies.</p>
42.	<p><a href="#">Fully Integrated Multi-Level Power Converter for SRM Drive with Charging Capabilities (G2V) for Electric Vehicle Application</a></p>

	<p><a href="#">V Shah, S Payami - IEEE Journal of Emerging and Selected Topics in Industrial Electronics, 2022</a></p> <p><b>Abstract:</b> The article presents a fully integrated multi-level power converter topology (IML-PCT) with integrated battery charging capability for switched reluctance motor (SRM) drive. The battery charger is integrated within the IML-PCT, which eliminates the requirement of any additional module for charging purposes. The proposed IML-PCT applies higher energization and de-energization voltages during the driving mode, which leads to an enhanced constant torque region for SRM drive. For battery charging mode, the proposed IML-PCT exhibits the characteristics of an on-board charger (OBC) capable of charging BESS directly via a standard AC outlet. The OBC functionality is realized by reconfiguring the proposed IML-PCT into an interleaved bridgeless boost power factor correction circuit (IBB-PFCC). The charging inductors for IBB-PFCC are realized by reutilizing/reconfiguring all the windings of the 4-phase SRM. Also, with the proposed IBB-PFCC configuration, the charging current in the windings leads to an average zero torque production. Thus, the rotor is kept stationary during battery charging mode without any external braking mechanism. Detailed simulation and experimental studies on a 1.1 kW laboratory prototype 4-phase SRM demonstrate AC level-1 (120V/240V) charging performance of the proposed IML-PCT.</p>
43.	<p><a href="#">Generic Multispectral Image Demosaicking Algorithm and New Performance Evaluation Metric</a>  <a href="#">V Rathi, P Goyal - International Conference on Computer Vision and Image Processing, 2022</a></p> <p><b>Abstract:</b> Color image demosaicking is key in developing low-cost digital cameras using a color filter array(CFA). Similarly, multispectral image demosaicking can be used to develop low-cost and portable multispectral cameras using a multispectral filter array (MSFA). In this work, we propose a generic multispectral image demosaicking algorithm based on spatial and spectral correlation. We also propose a new image quality metric Average-Normalized-Multispectral-PSNR (ANMPSNR), which helps in easily comparing the relative performance of different demosaicking algorithms. In experimental results, we prove the efficacy of the proposed algorithm using two publicly available datasets as per different image quality metrics.</p>
44.	<p><a href="#">Highlighting the corrosion mechanisms of corroded plain carbon steels using the atomic force microscopy</a>  <a href="#">PK Katiyar, R Maurya, PK Singh – 2022</a></p> <p><b>Abstract:</b> The focus of the present study is to examine the effect of the fraction of pearlite, the role of interlamellar spacing, and the pearlite colony size on the corrosion behavior of different carbon steels (0.002%C, 0.17%C, 0.43%C, and 0.7%C) and four different variants (coarse, medium, fine, and very fine) of 0.7%C pearlite steels. All the microstructures have been developed using suitable heat treatment processes and the polarization tests were carried out in a 3.5% NaCl solution. The corrosion mechanisms and extent of dissolution of all the steel specimens have been discussed with the aid of AFM (Atomic Force Microscopy) topographic images and found that the overall corrosion rate has mainly been governed by the combined action of the fraction of pearlite, pearlite colony size, interlamellar spacing and fineness of the microstructures. The extent of dissolution of the various constituents phases has also been examined by section analysis using the AFM images. Therefore, this technique can be employed to signify the differential micro-dissolution behavior of the different fineness of the microstructures as well as various constituents phases present in the corroded steel.</p>

45.	<p><a href="#">High-Speed Interconnects: History, Evolution, and the Road Ahead</a>  VR Kumbhare, R Kumar, MK Majumder, S Kumar, R Sharma.. - IEEE Microwave Magazine, 2022</p> <p><b>Abstract:</b> An integrated circuit (IC), or chip, is a set of electronic circuits and components placed on a tiny planar silicon (Si) semiconductor substrate. These electronics circuits and components are electrically connected to one another with the help of planar and vertical conductor elements known as interconnects. This article presents a detailed overview of the evolution of interconnects, highlighting the technological milestones that have been achieved during the past four decades. Interconnects form the backbone of signal communication among devices on a chip and between chips on a printed circuit board (PCB). The layout and design of interconnects on an IC are vital to the chip's performance, functionality, reliability, efficiency, and overall fabrication yield.</p>
46.	<p><a href="#">Ionic Liquid-Mediated One-Pot 3-Acylimino-3 H-1,2-dithiolo Synthesis from Thiocarboxylic Acids and Alkynyl nitriles via In Situ Generation of Disulfide Intermediates</a>  C Kumari, A Goswami - Journal of Organic Chemistry, 2022</p> <p><b>Abstract:</b> A practical and straightforward strategy for the synthesis of 3-acylimino-3H-1,2-dithiol derivatives via a metal-free annulation reaction of alkynyl nitriles with thiocarboxylic acids mediated by ionic liquids [BMIM]Br has been reported. This operationally simple protocol offers an easy and rapid access to a library of dithiol derivatives in moderate to good yields. The mechanistic studies show a benzoyldithio anion addition to alkynyl nitriles followed by an annulation reaction through the involvement of a disulfide moiety as the key intermediate.</p>
47.	<p><a href="#">Is 3D surface structuring always a prerequisite for effective SERS?</a>  Shinki, S Sarkar - Surfaces and Interfaces, 2022</p> <p><b>Abstract:</b> In this work, we systematically investigate and compare the need for 3D vis-à-vis 2D surface morphologies of SERS templates by considering all major aspects of uniformity, reproducibility, sensitivity and cost-effectiveness. Controlled Si nanostructured surfaces varying largely in their local height fluctuations are fabricated by adopting an effortless wet chemical etch process. To evaluate the SERS behavior, an Au (50%)-Ag (50%) alloy plasmonic layer is grown over these substrates owing to its high and stable SERS response. An initial assessment of the SERS activity is done by using Rh6G as a probe molecule. Apparently, the surface with 3D morphology shows a slightly higher response than the surface possessed with a few nm of surface roughness (2D). But from signal uniformity and reproducibility considerations the 2D morphology gives the lowest value of RSD of 5.56% in contrast to a high value of 27.13% for the 3D morphology. The 2D substrate also allows a LOD up-to <math>10^{-15}</math> M and an EF of <math>7.1 \times 10^7</math>, thereby indicating a high sensitivity at par the best values reported till date. Further, detection of methylene blue and methyl parathion up to nM concentrations bear testimony to its universal applicability and ultra-sensitivity.</p> <p><b>Graphical Abstract:</b></p> 



48.	<p><a href="#">Joint Trajectory and Velocity-Time Optimization for Throughput Maximization in Energy Constrained UAV</a>  N Gupta, S Agarwal, D Mishra - IEEE Internet of Things Journal, 2022</p> <p><b>Abstract:</b> In this paper, we aim to study an unmanned aerial vehicle (UAV)-assisted Internet-of-Things (IoT) communication system where a rotary-wing UAV travels from the initial to the final location to communicate with multiple IoT ground devices. The limited onboard energy of the UAV pose a constraint to the overall system's performance. UAV's energy consumption is majorly based on its kinematics, i.e., UAV's velocity and acceleration. Therefore, in this work, we maximize the sum user throughput by jointly optimizing the three-dimensional (3D) UAV trajectory, and velocity-time profile in the presence of onboard energy, velocity, acceleration and completion time constraints. Noting the non-convexity of the optimization problem, the original problem is decoupled into two sub-problems. First, the trajectory is optimized considering the velocity constraint, while in the second sub-problem, the velocity and time optimization in each time slot is carried out. Simulation results show insights on the UAV trajectory and velocity-time profile with the variation in the onboard energy availability. In addition, we demonstrate the superior performance of the proposed approach in comparison to the benchmark schemes.</p>
49.	<p><a href="#">Laser-assisted Turning of Aluminium 3003 Alloy</a>  N Deswal, R Kant – Lasers in Engineering, 2022</p> <p><b>Abstract:</b> Experimental work is performed to investigate the machinability of Al 3003 alloy by varying cutting speed and laser power during conventional turning and laser-assisted turning (LAT) with a fibre laser. The outcomes presented that the machining forces and surface roughness could be reduced significantly in LAT compared with conventional turning; however, machining forces and surface roughness were found to be increased during high laser power and low scan speed. Higher machining temperature is obtained during LAT than conventional turning due to extra heating by the laser at the workpiece surface. Low tool wear was observed at low cutting speed whereas high tool wear was obtained at high cutting speed in LAT than conventional turning. Higher chip segmentation frequency is obtained during LAT compared to conventional turning. The presented results are important for manufacturing industries seeking to enhance the machinability of the materials.</p>
50.	<p><a href="#">Multidirectional weighted interpolation based generic demosaicking for single-sensor multispectral imaging systems</a>  V Rathi, P Goyal - Digital Signal Processing, 2022</p> <p><b>Abstract:</b> Single-sensor based multispectral imaging systems with the multispectral filter array (MSFA) are the low-cost and portable means of capturing multispectral images (MSIs) having applications in different domains. These systems require an effective multispectral image demosaicking (MSID) method to reconstruct the full MSI from the raw image captured using single sensor. The MSFA patterns are also crucial for selecting the number of bands in the MSI and for the efficacy of MSID methods, and binary tree-based MSFAs (BT_MSFA) are preferred and widely used. Highlighting strong similarity in the pixel arrangements of bands with similar probability of appearance in the BT_MSFA, we propose a new generic MSID method based on the local multidirectional gradients and a weighted combination of spectral differences to find the missing pixel values of the bands. Experimental results confirm that the proposed MSID consistently outperforms the existing generic MSID methods in terms of various subjective and</p>

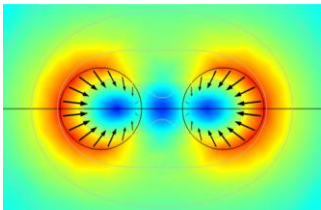
	objective image quality metrics on the three benchmark MSI datasets.
51.	<p><a href="#">Multi-parameter Wearable Band for Wireless Data Collection from People with Epilepsy</a>  HK Chattar, B Basumatary, R Shukla, BS Paul, R Kaur., AK Sahani.. - 2022 IEEE International Instrumentation and Measurement Technology Conference (I2MTC), 2022</p> <p><b>Abstract:</b> Epilepsy is a chronic non-communicable neurological disorder characterized by recurring seizures. People with epilepsy should be kept under constant surveillance because seizures can happen anywhere and anytime. Surveillance is required so that seizure events can be detected and the caregiver can be alerted. With the caregiver's intervention, chances of injury and death i.e Sudden Unexpected Death in Epilepsy (SUDEP) can be reduced. The seizure event should be recorded so that the doctors get insights into the patient's condition and the effect of prescribed anti-epileptic drugs (AEDs) based on the recorded data. Most of the available devices in the market use a limited number of sensors and are costly. Some devices use electrodes to record EEG and EMG data which are uncomfortable for the patient for continuous use. Hence, there is a need for a low-cost solution for seizure monitoring. Therefore, we have designed a low-cost microcontroller-based multi-parameters wearable band that senses some well-known biomarkers of seizure and sends data to the mobile application for further processing.</p>
52.	<p><a href="#">Multi-Response Optimization of Process Parameters to Minimize Geometric Inaccuracies in the Single Point Incremental Forming Process</a>  N Kumar, A Agarwal - Metal Forming Processes, 2022</p> <p><b>Abstract:</b> The incremental sheet metal forming (ISMF) process has been one of the developments in the field of conventional sheet metal forming processes and is normally ideal for making customized parts. The formation of components without component-specific dies/tools in ISMF provides a competitive alternative for producing low-volume sheet metal components economically and efficiently. Single point incremental forming (SPIF) is a solely die-less process and simple version of ISMF technology for manufacturing sheet material components. In this chapter, average radial error (mm), springback (<math>^{\circ}</math>), and pillow effect (mm) have been considered as main discrepancies that occurred in part formed by the SPIF process. A comparison between ideal CAD geometry and the formed part was made to predict the geometrical errors. Taguchi method-based design of experiments, the L16 orthogonal array, was employed to carry out the experiments on the developed SPIF setup. The process parameters were optimized for better responses based on the acquired results, as explained in the chapter. Multi-response optimization based on utility theory and the Taguchi method was utilized. The unified response consisting of three response parameters was expressed as a common index (utility) and studied for the optimal setting using the Taguchi approach.</p>
53.	<p><a href="#">Novel use of ultrasonic-assisted turning in conjunction with cryogenic and lubrication techniques to analyze the machinability of Inconel 718</a>  J Airao, CK Nirala, N Khanna - Journal of Manufacturing Processes, 2022</p> <p><b>Abstract:</b> Industries have been pursuing a competent machining system that meets the necessity of sustainability without deteriorating tool wear or final part quality of components made from difficult-to-cut material 'Inconel 718'. In this regard, a novel study, applying ultrasonic vibration along with lubrication (MQL) and cooling (LCO<sub>2</sub>) is proposed to enhance the machinability of Inconel 718. The purpose of this work is to examine the machinability of Inconel 718 in conventional and ultrasonic-assisted turning (UAT) under dry, wet, MQL, and LCO<sub>2</sub>. The</p>

	<p>experiments are performed on an in-house developed UAT setup, keeping all the machining parameters constant. The LCO<sub>2</sub> considerably reduces edge chipping, nose wear, adhesion, and abrasion wear in both the processes. Quantitatively, the conventional turning under LCO<sub>2</sub> reduces the flank wear by 32–60 %, power consumption by 4–41 %, and power consumption by 5–31 % compared to dry, wet, and MQL strategies. Similarly, the UAT under LCO<sub>2</sub> reduces the flank wear by 32–53 %, power consumption by 11–40 % and power consumption by 5–31 % compared to dry, wet, and MQL strategies. The UAT reduces the surface roughness and power consumption compared to conventional turning when used under MQL and LCO<sub>2</sub>. The LCO<sub>2</sub> in conjunction with ultrasonic vibration significantly reduces specific cutting energy and tool wear without compromising the surface quality. Moreover, the combination also helps in enhancing the chip breakability and reducing the strain localization. Ultimately, the UAT, along with LCO<sub>2</sub> promotes sustainability in the machining of Inconel 718.</p>
54.	<p><a href="#">NUMERICAL ANALYSIS OF THE PERFORMANCE OF ATMOSPHERIC WATER HARVESTING SYSTEM</a>  T Singh, R Beniwal, SK Das, H Tyagi - 7th Thermal and Fluids Engineering Conference (TFEC), 2022</p> <p><b>Abstract:</b> With the increasing water demand around the world, researchers are looking for new innovative techniques to meet this demand. Since available water resources are limited and only a few technologies like desalination are available which can be used to increase the water supply above the hydrological cycle to meet the rapidly increasing water demand. One such new emerging technology to increase the water supply is Atmospheric Water Harvesting (AWH), where the water vapors which are found everywhere in the air are condensed to obtain fresh water. The AWH system can run on low-grade energy like waste heat or solar energy, which is abundantly available in arid regions having water scarcity and can help in the decentralization of water resources by eliminating the need for power grids. In this paper, we have analyzed and compared some new innovative technologies of AWH systems after defining them mathematically and modeling them. The technologies will be compared based on various parameters such as the amount of water produced per day, the Gained Output Ratio (GOR) of the cycle under varying ambient conditions, such as dry bulb temperature (DBT), relative humidity (RH) and mass flow ratio (MFR). The results show that about 15kg<sup>h</sup><sup>-1</sup> of water may be harvested with a GOR of about 0.28 for 30°C DBT, 60%RH and 80°C desiccant inlet temperature.</p>
55.	<p><a href="#">Nutritional anemia: Patent landscape</a>  R Kaur, S Mishra, IV Nevolin, DR Choudhury, M Singh - World Patent Information, 2022</p> <p><b>Abstract:</b> Anemia is the World's disease of great attention that generally indicates low hemoglobin concentration in blood. The developing countries are the prime victims of the disease. The majority of scientific publications also focus on these regions. However, patent research focusing on applied developments instead of fundamental scientific results, related to the solution of this problem, cannot be found. Since nutrition is an essential factor in anemia prevention, this article explores the inventive activity in this particular subject area. Although the nature of work is more of an overview, it notes differences in inventions between Western and Eastern countries. The West is more active in medicine and treatment methods, while the East focuses on food technology, enzymes, and microorganisms that promote the absorption of nutrients. At the same time, Western inventions also receive comprehensive protection in Asian</p>

	<p>countries. Asian inventors, on the contrary, rarely disseminate their results on a wide scale as patenting is limited to national jurisdiction and have a lesser impact on the state-of-the-art. However, the cause for such difference between the regions remains an open question and cannot be answered adequately without incorporating additional factors. Undoubtedly, one should reject the income factor since China, Japan, and the Republic of Korea, are recognized as sources of innovations besides Western countries. Moreover, these Asian countries have sufficient resources for large-scale research in chemistry and pharmaceuticals.</p>
56.	<p><a href="#">On the Structure of Format Preserving Sets in the Diffusion Layer of Block Ciphers</a> T Chatterjee, A Laha, SK Sanadhya - IEEE Transactions on Information Theory, 2022</p> <p><b>Abstract:</b> In 2016, Chang et al. proposed a Format Preserving Encryption (FPE) scheme over a finite field and used an MDS matrix in the diffusion layer of the scheme for optimal diffusion. Later that year, Gupta et al. defined an algebraic structure named Format Preserving Set (FPS) is the diffusion layer of an FPE scheme. In 2018, Barua et al. showed that it is not possible to construct an FPS over a finite field in the diffusion layer of an FPE scheme if the cardinality of the set is not a power of prime. They extended the search of FPS over a finite commutative ring <math>R</math> and showed that if an FPS <math>S \subseteq R</math> is closed under addition then it gets module structure over some subring of <math>R</math>. Moreover, in this case, the only possible cardinalities of FPS are some power of the cardinalities of subrings when the module is free. The purpose of this article is twofold. Firstly, we show that it is possible to construct format preserving sets over a finite commutative ring which are not closed under addition. Secondly, we search for format preserving sets and MDS matrices over torsion modules. We provide examples of format preserving sets of cardinalities 26 and 52 over torsion modules and rings. These cardinalities are interesting because they correspond to the set of English alphabets, without and with capitalization. By considering a finite Abelian group as a torsion module over a PID, we show that a matrix <math>M</math> with entries from the PID is MDS if and only if <math>M</math> is MDS under the projection map on the same Abelian group.</p>
57.	<p><a href="#">Optoelectronic properties of 2D van der Waals heterostructure As/PtS<sub>2</sub> by first-principles calculations</a> A Patel, D Singh, Y Sonvane, PB Thakor - Materials Today: Proceedings, 2022</p> <p><b>Abstract:</b> In the recent work, the structural, electronic and optical properties of the 2D van der Waals heterostructure As/PtS<sub>2</sub> have been studied within the framework of the first-principles calculations. In the electronic properties, the band-structure and projected density of the van der Waals(vdW) heterostructure As/PtS<sub>2</sub> have been systematically examined. The heterostructure As/PtS<sub>2</sub> exhibits semiconducting nature with reduced electronic bandgap in comparison with pristine monolayer As and monolayer PtS<sub>2</sub>. The optical properties of heterostructure As/PtS<sub>2</sub> have been also investigated thoroughly. From the present investigation, the heterostructure As/PtS<sub>2</sub> is suggested as promising material for the optoelectronic applications at nano-scale.</p>
58.	<p><a href="#">Overview of the KUKA Robot Language-based Intelligent Algorithms on Industrial Robots for Multifaced Medical and Engineering Applications: A Modern Approach to Automation</a> H Garg, J Singh, A Kaushik, S Sharma, J Singh, G Singh - International Journal of Health Sciences, 2022</p> <p><b>Abstract:</b> Industrial robots have been in use for about fifty years. Typical applications of</p>

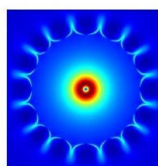
	<p>industrial robots include biomedical, painting, palletizing, welding, assembly, and material handling. As healthcare robotic systems for diagnostics, surgical treatments, or rehabilitative services: Robotic technologies seem to be very well with a broad array of applications in automation medical advancements. Apart from medical, an algorithm is designed to play electronic musical keyboards with the help of an industrial robot. The algorithm is implemented on the KUKA KR-16 industrial robot. The robot plays an electronic musical keyboard according to the keyboard notes of the desired song. The algorithm is designed to make the input of musical notes simple and easy. The design algorithm is further developed with KRL (KUKA Robot Language). The proposed algorithm results show that the KUKA KR-16 can play the specified notes.</p>
59.	<p><a href="#"><u>Parametric analysis to explore the viability of cold spray additive manufacturing to print SS316L parts for biomedical application</u></a>  A Singh, P Singh, BS Pabla, H Singh, S Shiva - Journal of the Brazilian Society of Mechanical Sciences and Engineering volume, 2022</p> <p><b>Abstract:</b> In the current work, high-pressure cold spray additive manufacturing (CS) is used to print SS316L samples to explore its potential as an AM technology for bio-implant applications. For comparison purposes, laser powder bed fusion (LPBF) is also used to print the samples. Porosity, microhardness, microstructure and young's modulus analysis of the printed materials were done. Subsequently, the influence of heat treatment on the characteristics of printed samples was analyzed after being subjected to two distinct kinds of heat treating environments, viz. cooling in air and furnace. The study results validated that the samples manufactured by the CS technique were more porous and rougher than the LPBF technique. Grain structure confirmed the presence of cellular sub-grains, dendrites, and melt pool boundaries in an as-fabricated LPBF sample. In as-fabricated CS, the microstructure consists of deformed multi-crystalline grains. Improvement in microhardness after heat treatment was observed in the LPBF samples, whereas CS exhibited less value because of the reduced effect of cold working. The heat treatment of CS samples with furnace cooling resulted in microhardness and Young's modulus comparable to that desired for the body implants. Therefore, this study opens a pathway to explore CS as a viable technique for manufacturing bio-implants with tailor-made porosity, hardness and Young's modulus by optimizing process parameters.</p>
60.	<p><a href="#"><u>PARAMETRIC STUDY ON THE PERFORMANCE OF AN ELECTROSTATIC PRECIPITATOR: A NUMERICAL APPROACH</u></a>  A Varshney, NK Mishra, R Das, GS Sinha - International Journal of Energy for a Clean Environment, 2022</p> <p><b>Abstract:</b> This paper presents the results obtained from numerical simulation of an electrostatic precipitator (ESP). In this study, detailed analysis of the ESP was completed based on different parameters. The main objective of this simulation was to calculate the effects of various parameters on the performance of the ESP, i.e., the collection efficiency, total number of accumulated charged particles, etc. The results showed that the applied voltage at the electrodes significantly influenced the collector's performance. At 25 kV, the collection efficiency reached 100% for 5 μm particle tracing and the total number of accumulated charged particles was <math>1.5 \times 10^4</math>. Furthermore, the results showed that the larger the size of the particle, the larger will be the collection efficiency and number of accumulated particles.</p>
61.	<p><a href="#"><u>Prediction of Mechanical Strength by Using an Artificial Neural Network and Random Forest</u></a></p>



	<p><a href="#">Algorithm</a>  K Upreti, M Verma, M Agrawal, J Garg, R Kaushik, C Agrawal.. - Journal of Nanomaterials, 2022</p> <p><b>Abstract:</b> Geopolymer concrete could be the best alternative to ordinary Portland cement concrete due to its higher performance in any severe condition. It reduces the carbon footprints to a very higher level. Machine learning methods are the future of the construction industry because it predicts the mechanical strengths of concrete mix design on the basis of their constituents without destructive test conduction. This study is aimed at developing the models to predict the mechanical strengths and validate them with the actual results. After the experimental investigation, we found the results of the mechanical (including compressive, splitting tensile, and flexural tensile) strength. The M2 mix of geopolymer concrete got the highest mechanical strengths whereas the M5 mix gets the lowest mechanical strengths among all the mix designs. The machine learning methods ANN (artificial neural network) and random forest are used to develop the models based on mixed experimental results. Mechanical strength results are taken as outputs, and mixed constituents are taken as inputs for training and testing. The performance of predicted results is checked based on , MAE (mean absolute error), RMSE (relative mean square error), RAE (relative absolute error), and RRSE (root-relative square error). Random forest models show the best prediction to the ANN models because it shows the negligible error between actual and predicted values. The value is 1 of 12 predicted results out of 15 by the use of random forest methods. So it is most suitable to predict the strength of geopolymer concrete based on their constituent’s material quantity.</p>
62.	<p><a href="#">Phenomenon in DC lines analogous to proximity effect</a>  A Kumar, CC Reddy - The European Physical Journal Plus, 2022</p> <p><b>Abstract:</b> It is casually assumed that charges are evenly distributed in conductors carrying direct current, unlike conductors carrying alternating current where proximity effect can be observed. The work negates this hypothesis through theoretical analysis and thoroughly conducted finite element simulations. All suspicions and expectations are validated affirmatively. A theoretical framework is developed to support the non-trivial findings, which conclusively establish the dependence of a transverse voltage on current in the conductor, distance between conductors, radius of the conductor, material, etc. and, most importantly, the occurrence of charge concentration in DC system. The exploration of the investigated phenomenon reveals deflection in electron path, which concentrates them toward one side, producing an effect in the DC system analogous to the proximity effect.</p> <p><b>Graphical Abstract:</b></p>  <p>The graphical abstract consists of two circular conductors positioned horizontally. Each conductor has a central blue dot with black arrows radiating outwards, representing electric field lines. The space between and around the conductors is filled with a color gradient from blue (low potential) to red (high potential), indicating the electric potential distribution. The field lines are more densely packed on the inner sides of the conductors, illustrating the proximity effect.</p>
63.	<p><a href="#">Pho(SC)-CTC—a hybrid approach towards zero-shot word image recognition</a>  R Bhatt, A Rai, S Chanda, NC Krishnan - International Journal on Document Analysis and Recognition, 2022</p>

	<p><b>Abstract:</b> Annotating words in a historical document image archive for word image recognition purpose demands time and skilled human resource (like historians, paleographers). In a real-life scenario, obtaining sample images for all possible words is also not feasible. However, zero-shot learning methods could aptly be used to recognize unseen/out-of-lexicon words in such historical document images. Based on previous state-of-the-art method for zero-shot word recognition “Pho(SC)Net”, we propose a hybrid model based on the CTC framework (Pho(SC)-CTC) that takes advantage of the rich features learned by Pho(SC)Net followed by a “connectionist temporal classification” (CTC) framework to perform the final classification. Encouraging results were obtained on two publicly available historical document datasets and one synthetic handwritten dataset, which justifies the efficacy of Pho(SC)-CTC and Pho(SC)Net.</p>
64.	<p><a href="#">Photoredox-Mediated Desulfonylative Radical Reactions: An Excellent Approach Towards C–C and C–heteroatom Bond Formation</a> I Chatterjee, B Paul, H Paul – <i>Synthesis</i>, 2022</p> <p><b>Abstract:</b> X (X= H or, heteroatom) bond formation.–C and C–In recent times, desulfonylative radical-cross-coupling (RCC) has come to the forefront in synthetic organic, bio, and material chemistry as a powerful strategy to forge C-C and C-heteroatom bonds. Diverse functionalization through metal and photoredox-catalyzed desulfonylation reactions has attracted the scientific community due to the mild reaction conditions, wide functional group tolerance and excellent synthetic efficacy. In this review, we have highlighted the photoredox-mediated desulfonylation reactions developed in the last two decades. The current review will summarize the newly reported methodologies, with particular emphasis on their mechanistic aspects and selectivity issues which have paved a new way towards sustainable C</p>
65.	<p><a href="#">Promise and reality of organic electrodes from materials design and charge storage perspective</a> A Banerjee, N Khossossi, W Luo, R Ahuja - <i>Journal of Materials Chemistry A</i>, 2022</p> <p><b>Abstract:</b> Organic electrode materials are becoming increasingly important as they reduce the C-footprint as well as the production cost of currently used and studied rechargeable batteries. With increasing demand for high-energy-density devices, over the past few decades, various innovative new materials based on the fundamental structure-property relationships and molecular design have been explored to enable high-capacity next-generation battery chemistries. One critical dimension that catalyzes this study is the building up of an in-depth understanding of the structure-property relationship and mechanism of alkali ion batteries. In this review, we present a critical overview of the progress in the technical feasibility of organic battery electrodes for use in long-term and large-scale electrical energy-storage devices based on the materials designing, working mechanisms, performance, and battery safety. Specifically, we discuss the underlying alkali ion storage mechanisms in specific organic batteries, which could provide the designing requirements to overcome the limitations of organic batteries. We also discuss the promising future research directions in the field of alkali ion organic batteries, especially multivalent organic batteries along with monovalent alkali ion organic batteries.</p>
66.	<p><a href="#">Radial viscous fingering induced by an infinitely fast chemical reaction</a> P Verma, V Sharma, M Mishra - <i>Journal of Fluid Mechanics</i>, 2022</p> <p><b>Abstract:</b> A numerical insight into the radial displacement of two viscously stable reactants undergoing an infinitely fast chemical reaction is obtained. This work broadens the numerical knowledge about the interaction between chemical reaction and hydrodynamic instability. A</p>

suitable transformation is utilised to deal with an infinite dimensionless parameter and reduce computational cost. Viscous fingering instability originates when the product has a different viscosity than the reactants. We calculate the onset time  $t_{on}$  when the instability begins to appear for different reactants by varying the log mobility ratio  $Rc/Rc$  and the Péclet number  $Pe/Pe$ . Based on  $t_{on}$ , we divide the time domain into stable and unstable zones with respect to instability. This helps to characterise reactants so as to have a flow with/without instability. For a fixed  $Pe/Pe$  and  $|Rc/Rc|$ , it is found that  $t_{on}$  is early for  $Rc > 0$  in contrast to the result for rectilinear displacement. This results in a wider stable zone for  $Rc < 0$ . Interestingly, it is found that the stable zone can be made independent of  $Pe/Pe$  by using a careful rescaling and we obtain the dependence of the onset time of instability on  $Rc/Rc$  and  $Pe/Pe$  as  $t_{on} \propto (|Rc|Pe^{\beta_1 - \beta_2})^{\beta_3}$  where the constant of proportionality and  $\beta_i$ ,  $i=1,2,3$ , depend upon the sign of  $Rc/Rc$ . In the unstable zone, we find that the length of the fingers depends upon the sign of  $Rc/Rc$ , which is not observed for any radial displacement of reactants undergoing a slow or moderately fast chemical reaction.



[Rational design of Cu\(I\)-anchored porous covalent triazine framework \(CTF\) for simultaneous capture and conversion of CO<sub>2</sub> at ambient conditions](#)

G Singh, CM Nagaraja - Journal of CO<sub>2</sub> Utilization, 2022

**Abstract:** The selective carbon capture and utilization (CCU) as a C1 source is sought to be an important step towards environmental remediation and sustainable production of useful chemicals. In this context, herein, we report the strategic integration of noble metal-free Cu(I) catalytic sites with a nitrogen-rich, CO<sub>2</sub>-philic, bipyridine functionalized covalent triazine framework (bipy-CTF) by a post-synthetic approach. The Cu(I)@bipy-CTF showed very good performance for simultaneous capture and fixation of CO<sub>2</sub> into  $\alpha$ -alkylidene cyclic carbonates ( $\alpha$ -aCCs), high-value commodity chemicals at ambient conditions. Further, the Cu(I) anchored bipy-CTF showed high CO<sub>2</sub> affinity with the interaction energy of 44.09 kJ/mol attributed to the presence of CO<sub>2</sub>-philic, basic nitrogen sites. The presence of both CO<sub>2</sub>-philic nitrogen and alkynophilic Cu(I) sites decorated in the 1D channels of bipy-CTF provided a good catalytic activity for the chemical fixation of carbon dioxide from dilute gas (13 % CO<sub>2</sub>) to yield  $\alpha$ -aCCs at atmospheric pressure (balloon) of CO<sub>2</sub>. Notably, Cu(I)@bipy-CTF showed high recyclability and chemical stability for multiple catalytic cycles. Overall, the present work represents a rare example of a COF-based recyclable catalyst for CO<sub>2</sub> fixation from dilute gas into valuable chemicals under mild conditions.

**Graphical Abstract:**

A rational construction of a bifunctional catalyst by anchoring catalytic noble metal-free Cu(I) catalytic sites in CO<sub>2</sub>-philic covalent triazine framework (CTF) for selective capture and conversion of CO<sub>2</sub> to high-value commodity chemical,  $\alpha$ -alkylidene cyclic carbonates ( $\alpha$ -aCCs) at ambient conditions is presented



68.	<p><a href="#">Service Duration Maximization for Continuous Coverage in UAV-Assisted Communication System</a>  J Dandapat, N Gupta, S Agarwal, S Darshi - IEEE Communications Letters, 2022</p> <p><b>Abstract:</b> This letter studies a UAV-assisted communication design where a rotary-wing UAV is launched to provide continuous coverage to mobile nodes. We aim to maximize the service time duration of the UAV by optimizing its three-dimensional (3D) trajectory while simultaneously ensuring adequate coverage to mobile nodes. Considering the limited energy available with the UAV, we frame an equivalent energy consumption minimization problem. Though the formulated problem is non-convex, it is shown that it is pseudoconvex under horizontal and vertical UAV coordinates. Based on this observation, we use alternating optimization to solve the problem. Numerical results provide trajectory insight and compare the service duration to the mobile nodes with different schemes.</p>
69.	<p><a href="#">Stability Analysis of Nanoscale Copper-Carbon Hybrid Interconnects</a>  B Kumari, R Sharma, M Sahoo - 2022 IEEE 72nd Electronic Components and Technology Conference (ECTC), 2022</p> <p><b>Abstract:</b> Copper Carbon (Cu-Carbon) hybrid interconnect is a new and an extremely promising candidate for future VLSI circuit applications, so it needs to be analyzed for not only propagation delay but its stability should also be examined in order to consolidate its claim as an alternative to existing interconnect configurations. In this work, stability analysis of the recently proposed Cu-Carbon hybrid interconnect is performed and compared with existing alternate hybrid interconnect candidates (i.e. copper, copper-graphene hybrid and copper-carbon nanotube composite). A three-line coupled interconnect system for 7 nm technology node is considered in this study whose dimensional parameters are adopted as per the IRDS roadmap guidelines. The unit-step response of Cu-Carbon hybrid interconnect is steepest as compared to others because of its lowest switching delay. Cu-Carbon hybrid appears to be the most stable as its nyquist plot intersects farthest from the critical point <math>(-1, j0)</math> towards origin. The effect of crosstalk leads to undershoots as seen in the time domain response of copper interconnects, but it does not have any notable effect on Cu-Carbon hybrid interconnects. It is evident that as the fraction of carbon nanotube in Cu-Carbon hybrid (<math>F_{cnt}</math>) increases, bandwidth increases due to decrease in resistance. Also, Cu-Carbon with <math>F_{cnt} = 0.8</math> is most stable amongst all configurations. We conclude that Cu-Carbon hybrid is the most stable candidate among all the alternative interconnect configurations, claiming it to be a desirable interconnect alternative for near-future VLSI applications.</p>
70.	<p><a href="#">Strategic Design of Mg-Centered Porphyrin Metal–Organic Framework for Efficient Visible Light-Promoted Fixation of CO<sub>2</sub> under Ambient Conditions: Combined Experimental and Theoretical Investigation</a>  R Das, SS Manna, B Pathak, CM Nagaraja - ACS Applied Materials &amp; Interfaces, 2022</p> <p><b>Abstract:</b> The sunlight-driven fixation of CO<sub>2</sub> into valuable chemicals constitutes a promising</p>

	<p>approach toward environmental remediation and energy sustainability over traditional thermal-driven fixation. Consequently, in this article, we report a strategic design and utilization of Mg-centered porphyrin-based metal–organic framework (MOFs) having relevance to chlorophyll in green plants as a visible light-promoted highly recyclable catalyst for the effective fixation of CO<sub>2</sub> into value-added cyclic carbonates under ambient conditions. Indeed, the Mg-centered porphyrin MOF showed good CO<sub>2</sub> capture ability with a high heat of adsorption (44.5 kJ/mol) and superior catalytic activity under visible light irradiation in comparison to thermal-driven conditions. The excellent light-promoted catalytic activity of Mg–porphyrin MOF has been attributed to facile ligand-to-metal charge transfer transition from the photoexcited Mg–porphyrin unit (SBU) to the Zr<sub>6</sub> cluster which in turn activates CO<sub>2</sub>, thereby lowering the activation barrier for its cycloaddition with epoxides. The in-depth theoretical studies further unveiled the detailed mechanistic path of the light-promoted conversion of CO<sub>2</sub> into high-value cyclic carbonates. This study represents a rare demonstration of sunlight-promoted sustainable fixation of CO<sub>2</sub>, a greenhouse gas into value-added chemicals.</p>
71.	<p><a href="#">Surface integrity in ultrasonic-assisted turning of Ti6Al4V using sustainable cutting fluid</a>  J Airao, CK Nirala, J Outerio, N Khanna - <i>Procedia CIRP</i>, 2022</p> <p><b>Abstract:</b> Titanium alloys have been commonly used in the aerospace and automotive industries because of their high strength-to-weight ratio and superior wear resistance. However, due to poor thermal conductivity, higher shear modulus, higher chemical reactivity, these alloys exhibit higher cutting forces, rapid tool wear and poor surface quality. Ultrasonic-assisted turning (UAT) has shown promising results in machining of Titanium alloys. In this article, an in-house developed UAT setup is used to analyze the surface integrity of Ti6Al4V under sustainable machining condition, i.e., vegetable oil-based cutting fluid (VCF). Input process parameters such as cutting speed, feed, depth of cut and tool geometries are kept constants. The surface integrity is analyzed in terms of surface roughness, surface topography, microhardness and microstructure. The results are compared for conventional turning and UAT under dry and VCF conditions. The results show a significant improvement in UAT under VCF condition due to an excellent lubrication property of Canola oil, promoting sustainability in the machining of Titanium Ti6Al4V.</p>
72.	<p><a href="#">Tempered stable autoregressive models</a>  N Bhootna, A Kumar - <i>Communications in Statistics - Theory and Methods</i>, 2022</p> <p><b>Abstract:</b> In this article, we introduce and study a one sided tempered stable first order autoregressive model called TAR(1). Under the assumption of stationarity of the model, the marginal probability density function of the error term is found. It is shown that the distribution of the error term is infinitely divisible. Parameter estimation of the introduced TAR(1) process is done by adopting the conditional least square and method of moments based approach and the performance of the proposed methods are evaluated on simulated data. Also, we study an autoregressive model of order one with tempered stable innovations. Using appropriate test statistic it is shown that the model fits very well on real and simulated data. Our models generalize the inverse Gaussian and one-sided stable autoregressive models existing in the literature.</p>
73.	<p><a href="#">Toward Avoiding Misalignment: Dimensional Synthesis of Task-Oriented Upper-Limb Hybrid Exoskeleton</a>  S Gupta, A Agrawal, E Singla - <i>Robotics</i>, 2022</p>



	<p><b>Abstract:</b> One of the primary reasons for wearable exoskeleton rejection is user discomfort caused by misalignment between the coupled system, i.e., the human limb and the exoskeleton. The article focuses primarily on the solution strategies for misalignment issues. The purpose of this work is to facilitate rehabilitative exercise-based exoskeletons for neurological and muscular disorder patients, which can aid a user in following the appropriate natural trajectory with the least amount of misalignment. A double four-bar planar configuration is used for this purpose. The paper proposes a methodology for developing an optimum task-oriented upper-limb hybrid exoskeleton with low active degrees-of-freedom (dof) that enables users to attain desired task space locations (TSLs) while maintaining an acceptable range of kinematic performance. Additionally, the study examines the influence of an extra restriction placed at the elbow motion and the compatibility of connected systems. The findings and discussion indicate the usefulness of the proposed concept for upper-limb rehabilitation.</p>
74.	<p><a href="#">Transition metal substituted MoS<sub>2</sub>/WS<sub>2</sub> van der Waals heterostructure for realization of dilute magnetic semiconductors</a>  SM Kumar, AJ Kumar, NK Sharma, S Sahoo, MC Sahu, SK Gupta, R Ahuja, S Sahoo - Journal of Magnetism and Magnetic Materials, 2022</p> <p><b>Abstract:</b> Atomically thin doped two dimensional (2D) layered materials manifest excellent magnetic features beneficial to the potential applications in spintronics. With the implementation of extensive first principles calculations, we demonstrate the MS<sub>2</sub> (M = Mo, W) monolayers, as well as their van der Waals (vdW) hetero-bilayers as promising candidates for the successful realization of 2D dilute magnetic semiconductors with the incorporation of Mn and Co dopants. Under various pairwise doping configurations at different host atom sites, we report the electronic properties modifications induced change in magnetic exchange interactions. The magnetic coupling among the dopant pairs can be tuned between FM and AFM orderings via suitable doping adjustments. The developed interlayer exchange coupling between the vdW layers leads to strong and long-ranged ferromagnetic interactions which unleash robust magnetic moments with stable doping configurations. Our findings address the novel magnetic behavior of the layered vdW heterostructures and may further guide the future experimental efforts for the possible applications in modern electronics and nanoscale magnetic storage devices.</p>
75.	<p><a href="#">Tree-Ring Isotopic Records Suggest Seasonal Importance of Moisture Dynamics Over Glacial Valleys of the Central Himalaya</a>  N Singh, M Shekhar, BR Parida, RK Tiwari - Frontiers in Earth Science, 2022</p> <p><b>Abstract:</b> Accelerated glacier mass loss is primarily attributed to greenhouse-induced global warming. Land–climate interactions have increasingly been recognized as an important forcing at the regional-local scale, but the related effects on the Himalayan glaciers are less explored and thought to be an important factor regulating spatial heterogeneity. The aim of the present study is a multi-decadal approximation of glacier—hydroclimate interaction over the western region of the central Himalaya (WCH). Multi-species, highly coherent, tree-ring cellulose δ<sup>18</sup>O chronologies from three sites across the WCH were used to derive atmospheric humidity (Atmospheric Moisture Content: AMC) record of the last four centuries. Annual-scale AMC reconstruction implies a decreasing regional atmospheric moisture since the mid-19th century and a sharp decline in recent decades (1960s). Coherency analyses between regional AMC and glacier mass balance (GMB) indicate an abrupt phase-shift in the relationship after the 1960s</p>

	<p>within a common record of the last 273 years. To ascertain the cause of this phase-shift, annual AMC was disintegrated into seasonal-scale, utilizing ~200 years of <math>\delta^{18}\text{O}</math> record of a deciduous tree species. Seasonal (winter: October–March; summer: April–September) AMC reconstructions and disaggregation results indicate higher sensitivity of regional ice-mass variability to winter moisture dynamics than summer. Winter season AMC reconstruction confirms a revival of winter westerlies-driven moisture influx in the region since the 1970 s. Meanwhile, the record for the summer season AMC indicates a gradual decline in moisture influx from the beginning of the 20th century. Interestingly, despite a prominent decline in Indian summer monsoon (ISM) precipitation after the mid-20th century, the summer season AMC—GMB relation remained stable. We hypothesize that decadal-scale greening, and consequently increased evapotranspiration and pre-monsoon precipitation might have been recycled through the summer season, to compensate for the ISM part of precipitation. However, isotope-enabled ecophysiological models and measurements would strengthen this hypothesis. In addition, high-resolution radiative forcing and long-term vegetation greening trends point towards a probable influence of valley greening on GMB. Our results indicate that attribution of ice mass to large-scale dynamics is likely to be modulated by local vegetation changes. This study contributes to the understanding of long-term hydroclimate—ice mass variability in the central Himalaya, where predictions are crucial for managing water resources and ecosystems.</p>
76.	<p><a href="#">Tuning the electronic, magnetic, and sensing properties of a single atom embedded microporous <math>\text{C}_3\text{N}_6</math> monolayer towards <math>\text{XO}_2</math> (X = C, N, S) gases</a> S Deshpande, M Deshpande, R Ahuja, T Hussain - <i>New Journal of Chemistry</i>, 2022</p> <p><b>Abstract:</b> Two-dimensional frameworks have attracted significant attention due to their great potential in many applications. Among the <math>g\text{-C}_x\text{N}_y</math> family, <math>\text{C}_3\text{N}_6</math> is one of the recently synthesized promising candidates, which exhibits semiconducting behavior. Motivated by its potential, we performed first-principles density functional theory (DFT) calculations to explore the structural, electronic, magnetic, and gas sensing properties of the <math>\text{C}_3\text{N}_6</math> ML towards common pollutants, such as <math>\text{XO}_2</math> (X = C, N, and S). We found weak binding between the pristine <math>\text{C}_3\text{N}_6</math> ML and <math>\text{XO}_2</math>, which was not suitable for efficient gas capture. However, functionalization with a selected transition metal not only altered the electronic and magnetic properties but also improved the sensing behavior of <math>\text{TM-C}_3\text{N}_6</math> (TM = Sc, Ti, V, Cr, Mn, Fe, Co, Ni, Cu, and Zn). We have analyzed the adsorption behavior, desorption time, and correlation matrix of TM embedded <math>\text{C}_3\text{N}_6</math> towards <math>\text{XO}_2</math> (X = C, N, and S) gases. Electronic structures and magnetic moments of <math>\text{XO}_2</math> adsorbed <math>\text{TM-C}_3\text{N}_6</math> depend on the atomic number of the embedded TM atom and the adsorbed gas molecules. We found that the adsorption energies of <math>\text{TM-C}_3\text{N}_6</math> systems towards <math>\text{NO}_2</math> gas molecules are stronger in comparison to <math>\text{CO}_2</math> and <math>\text{SO}_2</math> gas molecules, which suggested a selective capture mechanism. Based on our findings, <math>\text{TM-C}_3\text{N}_6</math> systems turned out to be promising adsorbent materials for environmentally toxic pollutants.</p>
77.	<p><a href="#">Tuning the interfacial chemistry for stable and high energy density aqueous sodium-ion/sulfur batteries</a> M Kumar, TC Nagaiah - <i>Journal of Materials Chemistry A</i>, 2022</p> <p><b>Abstract:</b> Low cost, highly safe, and environmentally benign aqueous rechargeable sodium-ion batteries (ARSIBs) are promising energy storage devices for the future. However, low cell voltage, low energy density, and inadequate cycling stability associated with low-capacity electrode materials, the restricted water stability window (1.23 V), and the inability of aqueous</p>

	<p>electrolyte to form a stable solid electrolyte interphase (SEI) is a major concern. In the present work, we have designed an aqueous rechargeable Na-ion/S battery, using a S@CoWO<sub>4</sub> anode coupled with a Na-W-U-D electrolyte prepared by mixing NaClO<sub>4</sub>, urea, and N,N-dimethylformamide (DMF) in water, that exhibits a remarkable stability window of 3.1 V due to reduced water activity and stable SEI formation. The excellent anchoring ability and accelerated polysulfide redox kinetics of CoWO<sub>4</sub> coupled with the high stability of Na-W-U-D electrolyte results in a very high capacity of 834 mA h g<sup>-1</sup> (w.r.t sulfur) at 0.5C with 88% retention after 500 cycles. Post stability XPS and SEM studies provide evidence of a smooth and stable SEI consisting of Na<sub>2</sub>CO<sub>3</sub>, polyurea, and reduced products of DMF, which prevent polysulfide dissolution and side reactions due to water electrolysis electrolyte evaporation and dissolved oxygen. Further, a full cell assembled by integrating the S@CoWO<sub>4</sub> anode and Na<sub>0.44</sub>MnO<sub>2</sub> cathode in the Na-W-U-D electrolyte shows remarkable durability and delivers an energy density of 119.0 W h kg<sup>-1</sup>, demonstrating the excellent potential of the cell for scale-up and manufacturing.</p>
78.	<p><a href="#">Unveiling two antiaromatic s-indacenodicarbazole isomers with tunable paratropicity</a>  HK Saha, D Mallick, S Das - <i>Chemical Communications</i>, 2022</p> <p><b>Abstract:</b> Linear and curved antiaromatic s-indacenodicarbazole isomers were synthesized and characterized to show the tunable paratropicity of s-indacene, as analyzed by NICS(1)zz and ACID (ring-current) calculations. The curved isomer showed a greater degree of antiaromaticity than the linear isomer, as predicted by the Glidewell-Lloyd rule. This degree of antiaromaticity was further validated by the red-shifted UV-vis absorption and smaller HOMO-LUMO energy gap.</p>

**Disclaimer:** This publication digest may not contain all the papers published. Library has compiled the publication data as per the alerts received from Scopus and Google Scholar for the affiliation “Indian Institute of Technology Ropar” for the month of July 2022. The author(s) are requested to share their missing paper(s) details if any, for the inclusion in the next publication digest.